Cannabinoid Receptor Type 1 Expression During Postnatal Development of the Rat Retina

N. Zabouri,[1,2] J.-F. Bouchard,[2] and C. Casanova[1]*

[1]Laboratoire des Neurosciences de la vision, École d'optométrie, Université de Montréal, Montréal, Québec, Canada H3C 3J7
[2]Laboratoire de Neuropharmacologie, École d'optométrie, Université de Montréal, Montréal, Québec, Canada H3C 3J7

ABSTRACT

Cannabinoid receptor type 1 (CB1R) participates in developmental processes in the central nervous system (CNS). The rodent retina represents an interesting and valuable model for studying CNS development, because it contains well-identified cell types with clearly established and distinct developmental timelines. Very little is known about the distribution or function of CB1R in the developing retina. In this study, we investigated the expression pattern of CB1R in the rat retina during all stages of postnatal development. Western blots were performed on retinal tissue at different time points between P1 and adulthood. In order to identify the cells expressing the receptor and the age at which this expression started, immunohistochemical co-staining was carried out for CB1R and markers of the different cell types comprising the retina. CB1R was already present at P1 in various cell types, i.e., ganglion, amacrine, horizontal, and mitotic cells. In the course of development, it appeared in cone photoreceptors and bipolar cells. For some cell types (bipolar, Müller, and some amacrine cells), CB1R was transiently expressed, suggesting a potential role of this receptor in developmental processes, such as migration, morphological changes, sub-identity acquisition, and patterned retinal spontaneous activity. Our results also indicated that CB1R is largely expressed in the adult retina (cone photoreceptors and horizontal, most amacrine, and retinal ganglion cells), and may therefore contribute to retinal functions. Overall these results indicate that, as shown in other structures of the brain, CB1R could play an instrumental role in the development and function of the retina. J. Comp. Neurol. 519:1258–1280, 2011.

INDEXING TERMS: endocannabinoids; CB1R; FAAH; immunohistochemistry; NAPE-PLD; retinogenesis

In the last two decades, there has been an increased interest in the physiological role of the endocannabinoid system and its main receptors, cannabinoid receptor types 1 (CB1R) and 2 (CB2R). CB1R has been predominantly studied, relative to CB2R, because of its ubiquitous presence in the central nervous system (CNS), including the retina (Herkenham, 1991; Mailleux et al., 1992; Westlake et al., 1994; Buckley et al., 1998; Straiker et al., 1999; Yazulla et al., 1999; Cravatt et al., 2001; Leonelli et al., 2005; Lalonde et al., 2006; Nucci et al., 2007; Warrier and Wilson, 2007). This receptor is a member of the superfamily of G protein-coupled receptors and is linked to $G_{i/o\alpha}$ proteins. These proteins inhibit most adenylyl cyclases and regulate calcium and potassium ion channels (see Turu and Hunyady, 2009 for review on CB1R signal transduction pathways).

Some constituents of the endocannabinoid system, i.e., ligands, synthesizing and degradative enzymes, and receptors, were found in different retinal cell types in several species, from fish to primates (Buckley et al., 1998; Straiker et al., 1999; Yazulla et al., 1999; Leonelli et al., 2005; Lalonde et al., 2006; Nucci et al., 2007; Warrier and Wilson, 2007; and see Yazulla, 2008 for review). For instance, in adult rodents, both CB1R and the enzyme fatty acid amide hydrolase (FAAH; responsible for hydrolyzing the CB1R ligand; Deutsch and Chin, 1993; Cravatt et al., 2001; McKinney and Cravatt, 2005) are expressed in cone photoreceptors (Straiker et al., 1999; Yazulla et al., 1999), bipolar (Yazulla et al., 1999), amacrine

Grant sponsor: Fonds de la recherche en santé (FRSQ) Vision Network and La fondation des maladies de l'oeit (to J.-F.B. and C.C.); Grant sponsor: Natural Sciences and Engineering Research Council (NSERC); Grant number: 194670-2009 (to C.C.); Grant sponsor: Canadian Institutes of Health Research (CIHR); Grant number: MOP-177796 (to J.-F.B.); Grant sponsor: CIHR-E.A. Baker Foundation scholarship (to N.Z); Grant sponsor: FRSQ Chercheur boursier junior 2 Foundation (scholar grant to J.-F.B).

*CORRESPONDENCE TO: C. Casanova, Laboratoire des Neurosciences de la vision, École d'optométrie, Université de Montréal, C.P. 6128 Succursale. Centre-Ville, Montréal, Québec, Canada H3C 3J7.
E-mail: christian.casanova@umontreal.ca

Received February 12, 2010; Revised June 29, 2010; Accepted September 28, 2010
DOI 10.1002/cne.22534
Published online October 19, 2010 in Wiley Online Library (wileyonlinelibrary.com)

(Yazulla et al., 1999; Warrier and Wilson, 2007), and retinal ganglion cells (RGCs; Straiker et al., 1999; Yazulla et al., 1999; Lalonde et al., 2006; Yazulla, 2008). Activation of CB1R can modulate ion currents in retinal cells of adult animals, suggesting the involvement of the endocannabinoid system in retinal processing (Straiker et al., 1999; Yazulla et al., 2000; Fan and Yazulla, 2003, 2007; Struik et al., 2006).

Most studies on CB1R expression were conducted in the retina of adult animals, and very little is known about its presence and role(s) in the developing retina. The paucity of information regarding CB1R expression in developing retinas is surprising given that endocannabinoids and their receptors are expressed very early in the CNS (embryonic day 13; Buckley et al., 1998) and are generally considered to play a role in developmental processes. Indeed, several lines of evidence indicate that endocannabinoids are involved in neurogenesis (Aguado et al., 2005; Galve-Roperh et al., 2006; Hill et al., 2006; Harkany et al., 2008), axonal elongation (Williams et al., 2003; Berghuis et al., 2005, 2007), and probably synaptogenesis (Kim and Thayer, 2001; Galve-Roperh et al., 2006; Berghuis et al., 2007; Gomez et al., 2007; Fride, 2008). To our knowledge, only three studies specifically investigated the endocannabinoid system in the retina of immature animals. In the embryonic chick retina, Leonelli et al. (2005) reported an early expression of the receptor in the retinotectal pathway, whereas Warrier and Wilson (2007) demonstrated a modulatory role of CB1R in the spontaneous release of γ-aminobutyric acid (GABA) in cultured amacrine cells. The third report revealed that activation of CB1R modified the excitability of cultured rat RGCs (Lalonde et al., 2006). These findings indicate that CB1R is present and functional early on at the retinal level.

In this study, we investigated the expression pattern of CB1R in the retina of young and adult rats. The rodent retina represents a valuable model for studying development because it contains several cell types with well-established and distinct developmental timelines (Rapaport et al., 2004). The specific aim was to determine the developmental profile of CB1R expression for each of the main retinal cell types, from birth to adulthood. Part of this work was presented in abstract form (Zabouri, 2007, 2008).

MATERIALS AND METHODS

Animals

Gestating or nongestating adult Long-Evans rats were obtained from Charles River (St-Constant, QC, Canada) and maintained on a 12-hour light/dark cycle. All procedures were in accordance with the guidelines set out by the Canadian Council on Animal Care and the U.S. National Institutes of Health guidelines for the care and use of laboratory animals, and were approved by the ethics committee on animal research of the Université de Montréal. Three to seven pups from at least three litters were used at every age for each co-labeling.

Tissue preparation

The animals were sacrificed at various ages, namely, P1, 3, 5, 7, 9, 11, 13, 15, 21, 30, 45 and adults (≥P60). Rats were deeply anesthetized either by hypothermia (pups younger than P5) or through excess of isoflurane inhalation. One eye was immediately removed for Western blot analysis. The retina was dissected on ice, promptly frozen, and kept at −80°C until further processing. Simultaneously, a transcardiac perfusion was conducted with phosphate-buffered 0.9% saline (PBS; 0.1 M, pH 7.4), followed by phosphate-buffered 2% paraformaldehyde (PFA), until the head was lightly fixed. The nasal part of the second eye was marked with a suture and removed. Two small holes were made in the cornea, prior to a first postfixation in 2% PFA for a period varying between 1 $^1/_2$ hours and 2 hours, depending on the size of the eye. The cornea and lens were then removed and the eyecups were postfixed for 10–30 minutes in 2% PFA. The degree of fixation was reduced to preserve the antigenicity of CB1R. The eyecups were washed in PBS, cryoprotected in 30% sucrose overnight, embedded in HistoPrep tissue Embedding Media (Fisher Scientific, Ottawa, ON), flash-frozen, and kept at −80°C until processing.

Sections (14 μm thick) were cut with a cryostat (Leica Microsystems, Exton, PA) starting at the nasal pole and placed on slides coated with either gelatin/chromium (double-frosted microscope slides, Fisher Scientific, Ottawa, ON) or poly-L-lysine (Sigma-Aldrich, Oakville, ON). The latter were used only when it was necessary to heat the samples for antigen retrieval.

Subcellular fractionation and Western blot

Subcellular fractionation

Freshly dissected retinas from adult rats were homogenized and divided into nuclear, cytoplasmic, and membrane fractions with a Nuclear Extract Kit (Active Motif, Carlsbad, CA), which was successfully used on retinal tissue by Leu and Ouyang (2006). In brief, retinas were homogenized and then successively incubated, vortexed, and centrifuged in detergent-containing hypotonic buffer, complete lysis buffer, and then RIPA buffer (Barker and Shooter, 1994). A protease inhibitor mixture (aprotinin, leupeptin, pepstatin [1:1,000] and phenylmethylsulfonyl fluoride [0.2 mg/ml]; Roche Applied Science, Laval, QC, Canada) was added to the buffers. Between each incubation, the supernatant, comprising the cytoplasmic, the nuclear, or the membrane fractions was removed and stored at −80°C until use. The insoluble pellet was then resuspended in each buffer described above until all fractions were collected. Protein

contents were equalized by using a Thermo Scientific Pierce BCA Protein Assay Kit (Fischer Scientific, Ottawa, ON, Canada). Thirty micrograms of protein/sample of the homogenate cytoplasmic, nuclear, and membrane fractions were resolved with 10% sodium dodecyl sulfate (SDS)-polyacrylamide gel electrophoresis, transferred onto a nitrocellulose membrane filter (BioTrace NT, Life Sciences, Pall, Pensacola, FL), blocked for 1 hour in 5% skim milk (Carnation, Markham, ON, Canada) in $TBST_{western}$ (0.15 M NaCl, 25 mM Tris-HCl, 25 mM Tris, 0.5% Tween-20), and incubated overnight with the primary antibodies, namely, anti-CB1R, anti-GAPDH, anti-NR2E3, and anti-GluR1. The last three antibodies were used to ensure the proper separation of the cytosol (Haque et al., 2008), the nuclei (Kanda and Swaroop, 2009), and the membranes (Xue et al., 2001), respectively.

The following day, the blot was exposed to the appropriate secondary antibody conjugated to horseradish peroxidase (1:5,000; Jackson ImmunoResearch, West Grove, PA) in blocking solution for 2 hours. Detection was carried out by using home-made ECL Western blotting detection reagents. Then membrane was air-stripped, reblocked, and exposed to a second primary antibody, until all proteins of interest were tested.

Evolution of CB1R overall expression in time, analyzed by Western blot

Retinas were homogenized by hand by using a sterile pestle in RIPA lysis buffer, supplemented with a protease inhibitor mixture. Samples were then centrifuged at 4°C for 10 minutes, and the supernatant was extracted and stored. Protein contents were equalized as previously described. Thirty micrograms of protein/sample were resolved with 10% SDS-polyacrylamide gel electrophoresis, transferred onto a nitrocellulose membrane, blocked for 1 hour, and incubated overnight with one of the following primary antibodies: rabbit anti-CB1R, rabbit anti-FAAH and rabbit anti-NAPE-PLD, rabbit anti-DAGLα, and mouse anti-GAPDH in blocking solution. The latter antibody was used to ensure the proper equalization and loading of all samples; the protein usually used for this (β-actin) was deemed inappropriate as it varies during development (Weinberger et al., 1996; Micheva et al., 1998).

Densitometric analysis was performed by using Scion (Frederick, MD) Image software (version 4.03) on scanned films obtained from a series of three independent Western blots, each performed with retinal samples from distinct experimental groups.

Immunohistochemistry

Double-label immunohistochemistry

Sections were washed in buffered saline (phosphate 0.1 M, 0.9% based saline was used), postfixed for 5 minutes in a 70% solution of ethanol, rinsed in 0.03% Triton X-100 buffered saline, and blocked in 10% normal donkey serum (NDS; Jackson ImmunoResearch) and 0.5% Triton X-100 in buffered saline for 1 hour. The sections were then co-incubated overnight in rabbit anti-CB1R solution with one of the following antibodies tagged as mouse and directed against: protein kinase C α (PKCα), syntaxin, glutamine synthetase (GS), Brn3, or proliferating cell nuclear antigen (PCNA). For the latter antibody, the buffer used consisted of a Tris 0.05 M, 0.9% based saline. The sections were then washed in buffered saline, blocked for 30 minutes, and incubated for 1 hour with the following secondary antibodies: Alexa donkey anti-rabbit 555 for CB1R and Alexa donkey anti-goat or mouse 488 for cell type markers (Molecular Probes, Eugene, OR). After washes, the sections were mounted with a home-made Dabco-PVD mounting medium (Ono et al., 2001).

Immunostaining of Brn3 required antigen retrieval and amplification protocols whereby the sections were incubated at 37°C for 30 minutes in a 0.06% $CaCl_2$ solution. After several washes, they were incubated in citric buffer (0.1 M, pH 6.0) at 80°C for 1 hour, and then allowed to cool to room temperature before proceeding with the rest of the protocol as previously described. A biotinylated anti-goat secondary antibody was used (Jackson ImmunoResearch), followed by 2 hours of incubation in avidin-biotin-peroxidase complex (ABC; Vectastain ABC Elite kit; Vector, Burlingame, ON, Canada) to ensure proper amplification of the signal. The latter was revealed with streptavidin coupled to fluorescein isothiocyanate (FITC, 1:200; Jackson ImmunoResearch, West Grove, PA).

All dilution factors for the antibodies, the immunogens, and the provenance of antibodies are provided in Table 1.

Sequential co-labeling immunohistochemistry

For these experiments, the sections were labeled in a serial manner. The exposition to the first primary antibody was conducted as previously described, followed by incubation for 1 hour in a goat anti-Fab fragment (Brandon, 1985; Jackson ImmunoResearch). This allowed us to tag the first primary antibody as a goat rather than a rabbit. The sections were revealed with secondary Alexa donkey anti-goat 488. Then, they were exposed to a second primary antibody overnight, the latter revealed with Alexa donkey anti-rabbit 555 the following day. This type of immunostaining has been previously used on retinal tissues by Sherry et al. (2003) as well as others. The markers that required this type of protocol were rabbit anti-recoverin (McGinnis et al., 1992a, 1997) and anti-cone-transducin (Johnson et al., 2001), co-labeled with rabbit anti-CB1R.

TABLE 1.
Antibodies Used in This Study

Antibody	Immunogen	Dilution[1]	Host	Company
CB1R	A fusion protein with the sequence MKSILDGLADTTFRTITTDLLYVGSNDIQYEDIK GDMASKLGYFPQKFPLTSFRGSPFQEKMTAGDNSPLVPAGDT of rat CB1R	H: 1/150 W: 1/1,000	Rabbit	C1233, Sigma-Aldrich, Oakville, ON, Canada
FAAH	Synthetic peptide from rat FAAH with the sequence ELCLRFMREVEQLMTPQKQPS	W: 1/500	Rabbit	101600, Cayman Chemical, Ann Arbor, MI
NAPE-PLD	Synthetic peptide from mouse NAPE-PLD with the sequence QSPAPSYQYPKETL	W: 1/3,000	Rabbit	NB110–80070, Novus Biologicals, Littleton, CO
DAGLα	The protein sequence CPAKQDELVISAR from the C terminus of human DAGLα	W: 1/2,000	Rabbit	IMG-30833, Imgenex, San Diego, CA
GAPDH	The full-length rabbit muscle GAPDH protein	W: 1/20,000	Mouse	G8795, Sigma-Aldrich
NR2E3	The full-length recombinant protein	W: 1/500	Rabbit	AB2299, Chemicon, Temecula, CA
GluR1	The C-terminus peptide sequence SHSSGMPLGATGL from the rat protein	W: 1/1,000	Rabbit	AB1504, Chemicon
Recoverin	The full-length recombinant human recoverin	H: 1/2,000	Rabbit	AB5585, Chemicon
Cone transducin ($G_{\alpha t2}$)	A synthetic peptide with the sequence IDYAEVSCVD from bovine retina	H: 1/200	Rabbit	Sc-390, Santa Cruz Biotechnology, Santa Cruz, CA
Syntaxin, clone HPC1	Synaptosomal plasma fraction of rat hippocampus	H: 1/500	Mouse	S0664, Sigma-Aldrich
PKC clone H7	A synthetic peptide with the sequence DFEGFSYVNPQFVHPILQSSV from the human protein[2]	H: 1/500	Mouse	Sc-8393, Santa Cruz Biotechnology
GS clone GS-6	The full protein purified from sheep brain	H: 1/3,000	Mouse	MAB302, Chemicon
Brn3 C-13	Synthetic sequence RQKQKRMKYSAGI from the human Brn3b protein (Poche et al., 2008)	H: 1/500	Goat	Sc-6026, Santa Cruz Biotechnology
PCNA clone PC10	Synthetic peptide with the sequence LVFEAPNQEK (Ino and Chiba, 2000)	H: 1/500	Mouse	M0879, Dako, Carpinteria, CA

[1]H, immunohistochemistry; W, Western blot.
[2]Based on the sequencing of the blocking peptide by tandem mass spectrometry.

Antibody characterization

The antibodies used against the proteins comprising the endocannabinoid system studied here (NAPE-PLD, DALGα, CB1R, and FAAH) have not been previously characterized. Consequently, we tested their specificity with Western blot by using adult rat retina lysates. The immunoblot analyses are presented in Figure 1A.

The anti-NAPE-PLD yielded a double band at around 50 kDa. The anti-DAGLα reacted with a single band at 120 kDa as described by the manufacturer and other authors (Suarez et al., 2008; Gao et al., 2010; Suarez et al., 2010).

The anti-CB1R reacted with a robust band at 53 kDa and several very light ones below. This could be due either to the presence of several isoforms of the protein or to some degradation bands. Yazulla et al. (1999) reported the presence of a larger band at 160 kDa and interpreted it as a dimer of CB1R in albino rats. We did not observe this band with retinal homogenates from Long-Evans rats. However, we did observe this band with mice homogenates (data not shown). This indicates that the presence of CB1R dimers may be species and/or strain specific. The specificity of the CB1R antibody was also verified by immunolabeling retinal tissue when the *cnr1* gene (the gene encoding for CB1R) was deleted ($cnr1^{-/-}$; Marsicano et al., 2002). These samples were generously provided by Dr Beat Lutz.

To ensure the closest possible match between wild-type and $cnr1^{-/-}$ C57BL/6J mice, Dr. Lutz provided tissue from both wild-type and knockout animals. Sections from both samples were processed together during the same experiment; pictures were taken under the same exact conditions, and off-line processing was identical. The results are shown in Figure 1B and C. The CB1R staining in wild-type animals yielded a clear signal throughout the retina (Fig. 1B), whereas no staining was visible in the knockout, with the exception of some feeble immunofluorescence in the GCL (Fig. 1C). We do not know whether this result is due to remnants of the CB1R protein containing the epitope or to some nonspecific staining. However, the intensity of immunoreactivity is extremely low when compared with that observed in wild-type animals and can therefore be considered negligible.

The antibody reacting with FAAH yielded a dense band at about 66 kDa and a very light one below 37 kDa. The other antibodies used have been previously characterized by others. NR2E3 protein is a photoreceptor-specific nuclear receptor that belongs to the nuclear hormone receptor superfamily of ligand-modulated transcription factors (Kobayashi et al., 1999). The antibody rabbit anti-NR2E3 (Chemicon, Temecula, CA) reacts with a major double bond at about 44 kDa (manufacturer's technical information). This specific antibody was used by Leu and

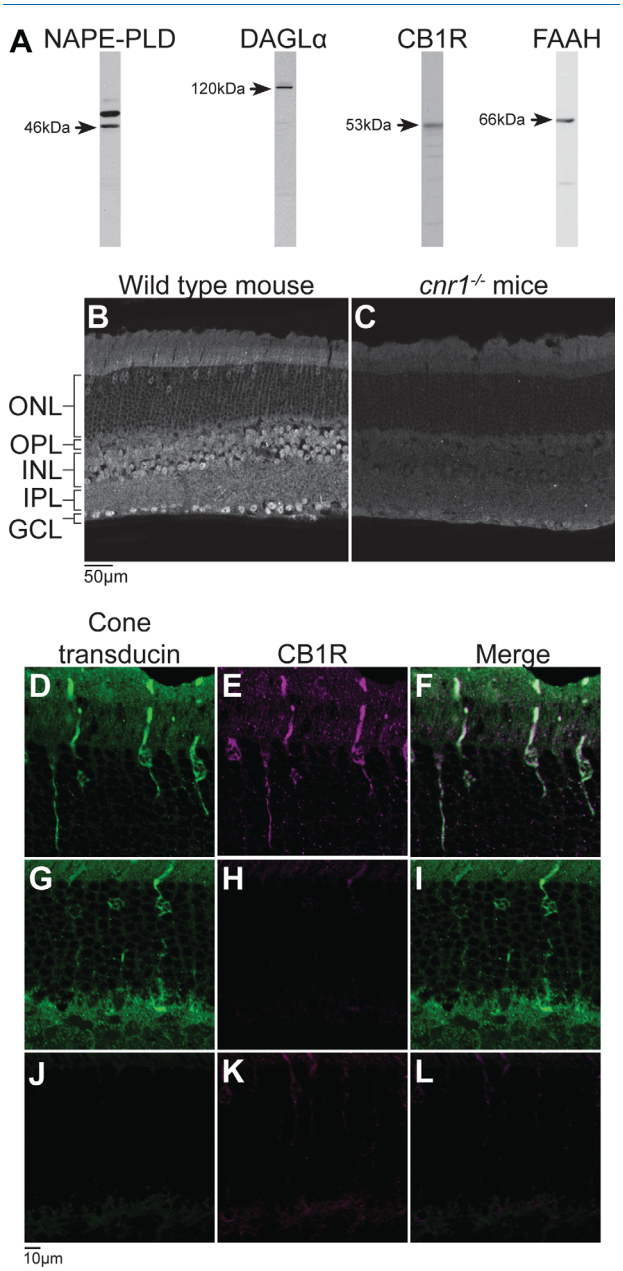

Figure 1. **A:** Immunoblots of NAPE-PLD, DAGLα, CB1R, and FAAH immunoreactivities in the rat retina. **B,C:** CB1R immunoreactivity in the retina of a wild-type and a *cnr1*$^{-/-}$ mouse. **D–L:** Cone-transducin (D,G,J) and CB1R (E,H,K) signals and their overlay (F,I,L) for the complete sequential protocol (D–F), for the control with the second primary antibody omitted (G–I), and for the control with the first secondary and second primary antibodies omitted (J–L). ONL, outer nuclear layer; OPL, outer plexiform layer; INL, inner nuclear layer; IPL, inner plexiform layer; GCL, ganglion cell layer. Scale bar = 50 μm below B (applies to B,C); 10 μm below J (applies to D–L).

Ouyang (2006) as a control for their retinal fractionation experiment.

GluR1 is expressed at the cell membrane and was used as a control for the proper separation of membranes during fractionation. Rabbit anti-GluR1 (Chemicon) was reported to react with the appropriate band at about 110 kDa by Nicholson and Geinisman (2009).

The mouse anti-GAPDH (clone GAPDH-71.1, Sigma, St. Louis, MO) reacted with a single band at about 37 kDa.

The protein PKCα is specifically expressed in rod bipolar cells and dopaminergic amacrine cells (Negishi et al., 1988). Mouse anti-PKCα (H7, Santa Cruz Biotechnology, Santa Cruz, CA) was shown to recognize rod bipolar cells exclusively (Gaillard et al., 2008). These authors as well as others also reported that this antibody recognizes PKCα, an 80-kDa protein (Nagar et al., 2009). The staining pattern we observed was similar to that reported in previous studies (Negishi et al., 1988; Ghosh et al., 2004; Gaillard et al., 2008; Morrow et al., 2008).

The protein syntaxin-1 was recognized as a specific marker of retinal amacrine and horizontal cells by several research teams (Barnstable et al., 1985; Nag and Wadhwa, 2001; Hirano et al., 2005; Li et al., 2010). Mouse anti-syntaxin (HPC-1; Sigma) recognized syntaxin-1, a 35-kDa protein, from hippocampal, retinal, and cortical neurons (Inoue et al., 1992). The staining pattern observed in the present study was similar to that previously reported (Li et al., 2004; Voinescu et al., 2009).

The expression of glutamine synthetase in Müller cells was demonstrated by Riepe and Norenburg (1977). Chang et al. (2007) established that the mouse anti-GS antibody (clone GS-6, Chemicon) reacted with a single 45-kDa protein in adult retinal tissue. The staining obtained with this antibody was comparable to that published elsewhere (Hojo et al., 2000; Gargini et al., 2007; Kim et al., 2008)

PCNA was chosen as a neuroblast and mitotic cell marker because it provides the least false-positive and -negative immunolabeling of neuroblasts and mitotic cells in the retina (Barton and Levine, 2008).The specificity of this mouse anti-PCNA (clone PC10, Dako, Carpinteria, CA) was fully characterized by Waseem and Lane (1990) and others (Ino and Chiba, 2000); it recognized a single band at 36kDa.

Anti-Brn3 was used to identify retinal ganglion cells. The Brn3 antibody (clone C-13, Santa Cruz Biotechnology) specifically recognizes three bands in Western blot corresponding to the three Brn3 family members, Brn3a at 53 kDa, Brn3b at 51 kDa, and Brn3c at 42 kDa (manufacturer's technical information). Its specificity for ganglion cells was demonstrated by Pan et al. (2005). The staining pattern obtained in the present study is similar to that found by others (Pan et al., 2005; Quina et al., 2005; Elshatory et al., 2007; Poche et al., 2008).

A number of laboratories have shown that recoverin is expressed in a subset of bipolar cells (Milam et al., 1993; McGinnis et al., 1997; Haverkamp and Wässle, 2000; Haverkamp et al., 2003). The immunoreactivity obtained

in our study with the rabbit anti-recoverin revealed a pattern of recoverin immunoreactivity identical to that described in the mouse retina (Haverkamp et al., 2003; Gargini et al., 2007; Acosta et al., 2008). This antibody (Chemicon) recognized a single 26-kDa band (manufacturer's technical information), in accordance with the reported size of recoverin (Yan and Wiechmann, 1997).

The rabbit anti-cone transducin-α subunit (Santa Cruz Biotechnology) was used to identify cone photoreceptors. The specificity of this antibody was confirmed by preadsorption and Western blot studies (Coleman et al., 2004); it recognizes a single band at 46 kDa.

Validity of the sequential labeling

Validity of the sequential staining was verified for CB1R/recoverin and CB1R/cone-transducin co-labeling with two controls: 1) the second primary antibody was omitted, yielding strong staining with the goat secondary 488 but no staining with rabbit secondary 555; and 2) the first secondary and second primary antibodies were omitted, yielding no signal for the goat secondary 488 and some low residual signal for the rabbit secondary 555. An example is presented in Figure 1D–L for CB1R and cone-transducin immunolabeling. The first line (Fig. 1D–F) shows immunostaining with the complete protocol: clear signals for both cone-transducin (Fig. 1D) and CB1R (Fig. 1E) can be seen, and this co-labeling shows that CB1R and cone-transducin signals overlap considerably (Fig. 1F). The second line (Fig. 1G–I) illustrates the result of the first control for the same co-immunolabeling. As expected, there is a clear signal for cone-transducin (Fig. 1G,I), whereas very little staining for CB1R is visible (Fig. 1H,I). The last line (Fig. 1J–L) presents the results for the second control, i.e., very little staining for both cone-transducin (Fig. 1J,L) and CB1R (Fig. 1K,L). Thus, these control data demonstrate that the sequential Fab fragment protocol remains specific even when there is a great deal of overlap between two proteins.

Confocal microscopy

Pictures of the central retina (within 200 μm of the optic nerve head) and the periphery were taken using a Leica TCS SP2 laser scanning confocal microscope (Leica Microsystems), with a 40× objective. Matching images were captured in the Alexa fluo 555/546 and Alexa fluo 488/FITC channels at a definition of 2,048 × 2,048 pixels, pseudo-colored, merged, and exported by using Leica LCS software (version 2.61). Throughout this study, retinal cell markers are always presented in green and CB1R is shown in magenta. The images were taken sequentially to ensure no "bleed-through" between channels. Images were selected to illustrate representative findings of the immunostaining at all ages studied. Pictures were pseudo-colored in magenta with Adobe Photoshop (CS4, Adobe Systems, San Jose, CA). Contrast and brightness were adjusted when necessary using the same software.

No differences were observed in CB1R expression between the center and the periphery of the retina, with the exception of the expected delay in development (Rapaport et al., 2004; and see Malicki, 2004 for review). Consequently, only pictures of the central retina are presented in the Results section.

When the co-expression of CB1R and retinal cell markers was ambiguous, the presence or absence of co-labeling was demonstrated by taking z-stacks with optimized steps. This allowed visualization of cells in the X-Y, X-Z, and Y-Z axes, thereby confirming the expression or the lack of CB1R in specific cell types. An example of such an analysis is shown in Figure 6U.

RESULTS

Temporal and spatial patterns of expression of CB1R and associated enzymes

Western blot analysis

We investigated the temporal pattern of expression of four elements of the endocannabinoid system in the retina by evaluating the total amounts of CB1R and endocannabinoid-synthesizing and degradative enzymes (NAPE-PLD, DAGLα, and FAAH, respectively) at various postnatal time points from P1 to adult. Representative examples of each protein expression across the different ages are presented in Figure 2A. The lower blot shows the expression of the protein GAPDH and demonstrates equal loading in all lanes. The averaged measures ± SEM, evaluated as the optical densities (ODs) of the bands, of CB1R, NAPE-PLD, DAGLα, and FAAH are shown in Figure 2B, C, D, and E, respectively. All these proteins varied across development and had different expression patterns. CB1R expression was fairly stable during the first 2 weeks. At the end of the second week, there was a sharp increase in expression that reached a plateau at P19 and remained stable throughout the next developmental stages. (P19, 21, 30, and 45 and adult were all significantly different from P1, Dunnett test, $P \leq 0.05$.)

The synthesizing and degradative enzymes did not exhibit the same pattern as CB1R. NAPE-PLD expression was decreased at P21 and reached a plateau at P30. (NAPE-PLD levels at P30 and P45 were significantly different from P1, Dunnett test $P \leq 0.05$.) DAGLα expression remained stable until P13, at which point it started to decrease, reaching a minimum level at P45. (DAGLα levels at P45 were significantly different from P1, Dunnett test $P \leq 0.05$.) The decrease in DAGLα concentration was extensive; it dropped by about half the amount

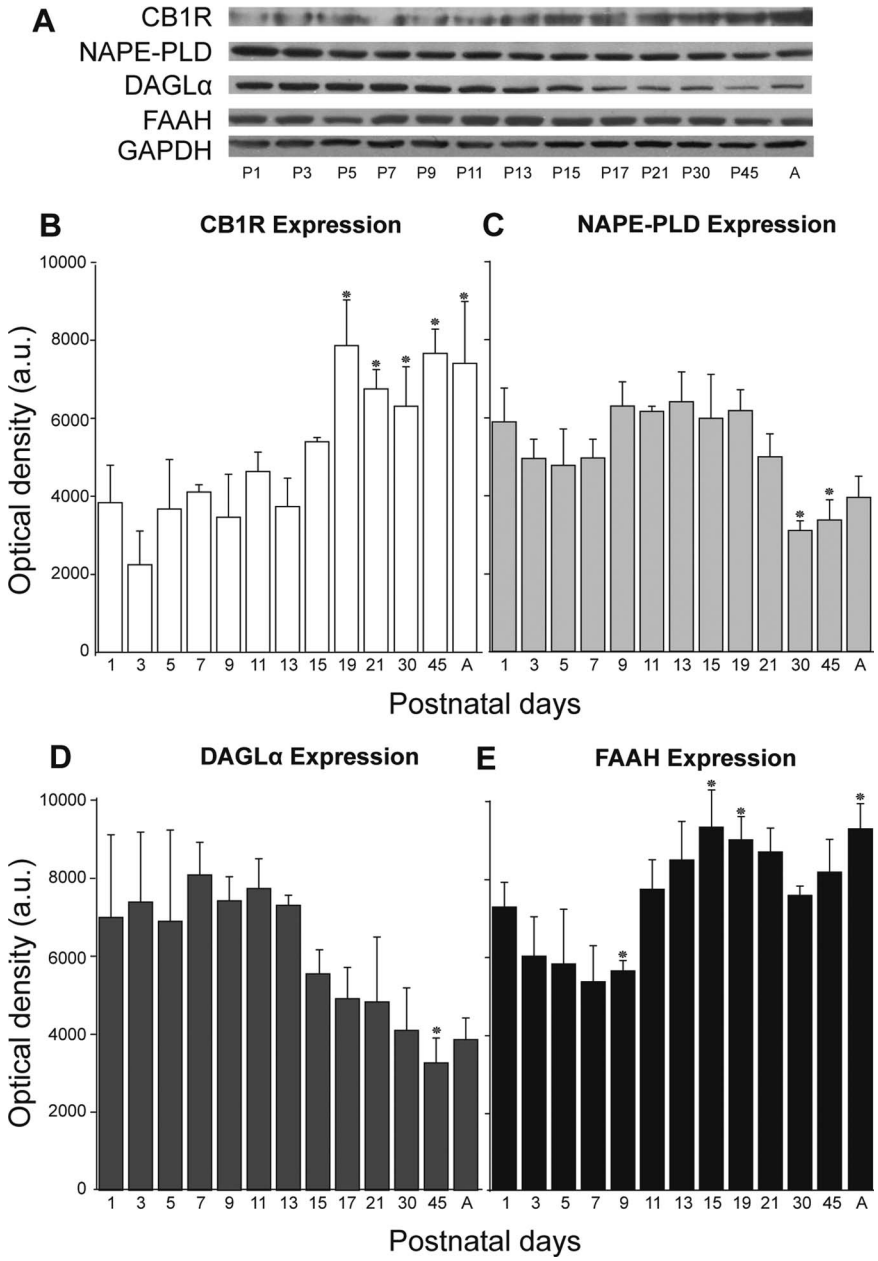

Figure 2. **A:** Representative examples of CB1R, NAPE-PLD, DAGLα, and FAAH expression during retinal development. **B–E:** Averaged variations of CB1R (□, B), NAPE-PLD (■, C), DAGLα (■, D) and FAAH (■, E) during retinal postnatal development and maturation as measured by Western blot analysis. Specific bands were seen at around 53 kDa for CB1R, 46 kDa for NAPE-PLD, 120 kDa for DAGLα, and 66 kDa for FAAH. Retinas were collected from rats between P1 and adult. The quantifications were performed on three different sets of samples. and mean optical densities± SEM in arbitrary units (a.u.) are presented for each age group. The statistical differences were assessed using a Dunnett test. *, Significant change compared with P1 ($P \leq 0.05$).

measured at P1. In contrast, the concentration of FAAH decreased over the first week of life, reaching a minimum at P9. (Its level was significantly different from P1, Dunnett test $P \leq 0.05$.) This was followed by an increase in FAAH concentration during the second and third weeks, reaching a maximum at P15. (FAAH: P15, P19, and adult levels were significantly different from P1, Dunnett test, $P \leq 0.05$.)

Immunohistochemistry

At birth, the retina is characterized by a neuroblast layer, and plexiform and ganglion cell layers (NBL, IPL, and GCL respectively). CB1R was already present: it was strongly expressed in the deepest and most superficial parts of the NBL, as well as in distinctive roundish cells located in the upper part of the NBL (Fig. 3A). The remaining parts of the NBL and the IPL showed some

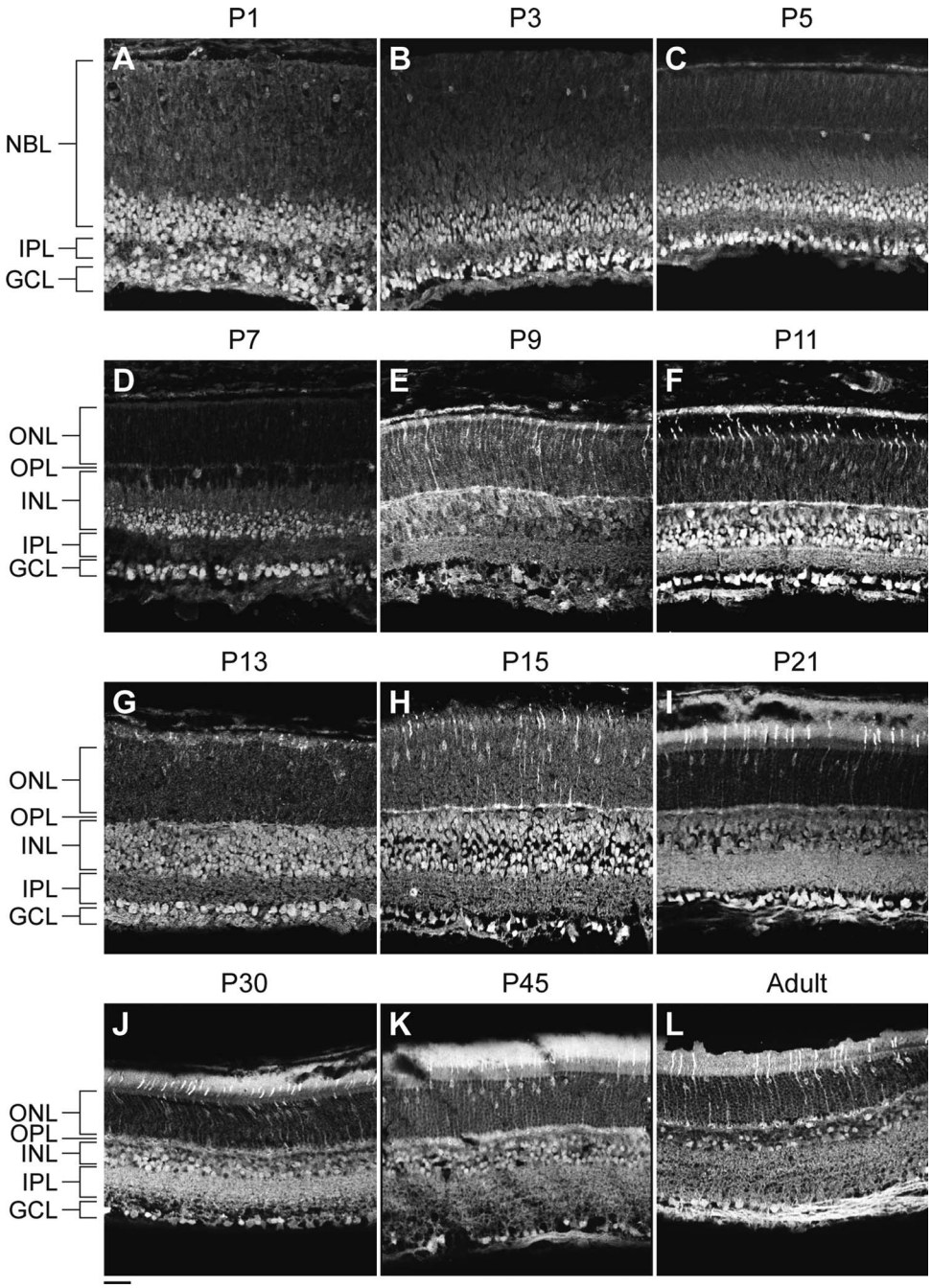

Figure 3. CB1R immunoreactivity in the developing rat retina. **A–L:** Vertical sections from P1 (A), P3 (B), P5 (C), P7 (D), P9 (E), P11 (F), P13 (G), P15 (H), P21 (I), P30 (J), P45 (K) and adult (L) rat retinas. For all ages, confocal images were obtained from a single focal plan. NBL, neuroblast layer; ONL, outer nuclear layer; OPL, outer plexiform layer; INL, inner nuclear layer; IPL, inner plexiform layer; GCL, ganglion cell layer. Scale bar = 40 μm below J (applies to A–L).

fluorescence, although it was not very pronounced. CB1R was strongly expressed in the GCL. A similar pattern of expression was observed at P3 (Fig. 3B).

Starting at P5, some photoreceptors in the forming ONL were immunopositive for CB1R. Based on their small number, these cells were suspected to be cones (Fig. 3C,D). A wave of CB1R expression appeared in the forming INL (Fig. 3C), reaching the most superficial part of this layer between P7 and P9 (Fig. 3D,E). This expression was of lower intensity than that of fully differentiated neurons located within the same layer. Around P7, there was also some immunofluorescence in the IPL and the forming OPL (Fig. 3D).

By P9, CB1R was found in the outer segment of cones as well as their cell bodies, axons, and synaptic pedicles (Fig. 3E), the latter accounting for the most intense

immunolabeling in the OPL. CB1R was also present in cells equally distributed just below the forming OPL, a pattern suggestive of horizontal cells. By P11, CB1R expression started to decrease and become more diffuse in the upper part of INL (Fig. 3F). In the IPL, the receptor expression increased, reaching a peak between P7 and P11, after which it decreased and remained stable over the rest of the period we studied.

By eye opening (P12–14), the retinal structure is basically complete, albeit still immature. During the weeks following eye opening, several maturation processes occur, including synapse consolidation or elimination and cell death. CB1R expression remained stable in the ONL and OPL throughout this period. In particular, it was strongly expressed in the outer and inner segments, cell bodies, axons, and synaptic pedicles of suspected cones (Fig. 3G–L). In the INL, however, several changes could be seen. At P15, most cells in this layer were CB1R immunofluorescent, the cells closer to IPL being more intensely stained than those closer to the OPL (Fig. 3H). By P21, the expression in the outer part of the INL became weaker and more diffuse, whereas it remained stable (i.e., strong) in its inner part (Fig. 3I). One week later, at P30, expression in the whole INL became sparse, as a number of cells throughout this layer turned immunonegative for CB1R (Fig. 3J). This expression profile was maintained over the following weeks (Fig. 3K) until adulthood, at which point only a few positive cells could be observed in the INL (Fig. 3L).

In the GCL, the expression of CB1R remained constant and high from P1 to adult.

Subcellular fractionation

Careful examination of the retina of wild-type mice (Fig. 1A) indicated an absence of CB1R expression in the nuclei of the cells. In the rat retina, however, CB1R immunolabeling appeared to be present in some nuclei of rat retinal cells (see, for example, Fig. 3L), which is surprising for a G-coupled protein receptor mainly implicated in neurotransmission modulation. To clearly establish the cellular compartments where CB1R was expressed, subcellular fractionation of adult rat retinas was conducted.

Three fractions were isolated: the cytosol, nuclei contents, and membranes. Separation of the fractions was verified by using GAPDH, NR2E3, and GluR1, respectively (Fig. 4). The fractionation experiments indicated that CB1R was present in cytosolic and membrane compartments, but not in the nuclei fraction (upper blot). Based on this finding, we propose that the observed CB1R expression in some nuclei most likely resulted from our tissue preparation procedure, which was characterized by light tissue fixation in order to preserve CB1R antigenicity. This sort of protein redistribution artifacts has been previously reported and associated with light fixation and permeabilization (Goldenthal et al., 1985; Melan and Sluder, 1992; Mayor and Maxfield, 1995; Cinar et al., 2006). The presence of this artifact has no impact on the study because we investigated CB1R expression within cell types rather than its subcellular distribution.

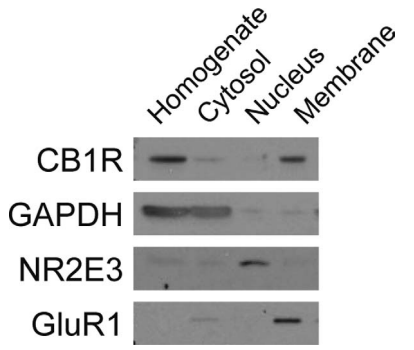

Figure 4. CB1R expression in different cell compartments in adult rat retina. The different cellular fractions were separated by successive centrifugations. Proper separation of the fraction was verified with GAPDH (cytoplasm), NR2E3 (nuclei), and GluR1 (membranes). CB1R was present in cytosol and membranes, but not in nuclei.

Cell types expressing CB1R

Early-born neurons

At birth, almost all horizontal, amacrine, and ganglion cells, as well as cone photoreceptors, are already differentiated (these neuron classes are called *early-born neurons*; Morest, 1970; Rapaport et al., 2004), the remaining ones being generated early after P0 (Rapaport et al., 2004). We investigated the presence of CB1R in these early-born neurons. Horizontal cells expressing CB1R could be distinguished at P1, as shown in Figure 5A–C (asterisks). The expression in these cells was robust in the cell body and absent from the immature processes. At P5–7, most horizontal cells reached their final position underneath the emergent OPL. At this stage, expression of CB1R was concentrated in the cell bodies (Fig. 5D–F) and remained so over the maturation period and into adulthood (Fig. 5G–U).

CB1R was also expressed in amacrine cells from P1 (Fig. 6A–C). Despite some variations in the intensity of immunolabeling, virtually all amacrine cells expressed CB1R until P15 (Fig. 6D–F). Of interest is the fact that some cells located for the most in the deepest part of the INL showed a transient expression of CB1R as they became immunonegative (Fig. 6G–I) at P15. CB1R-immunonegative amacrine cells were observed at every age after P15 and into adulthood (Fig. 6J–U). To clearly confirm the absence of CB1R from all parts of these

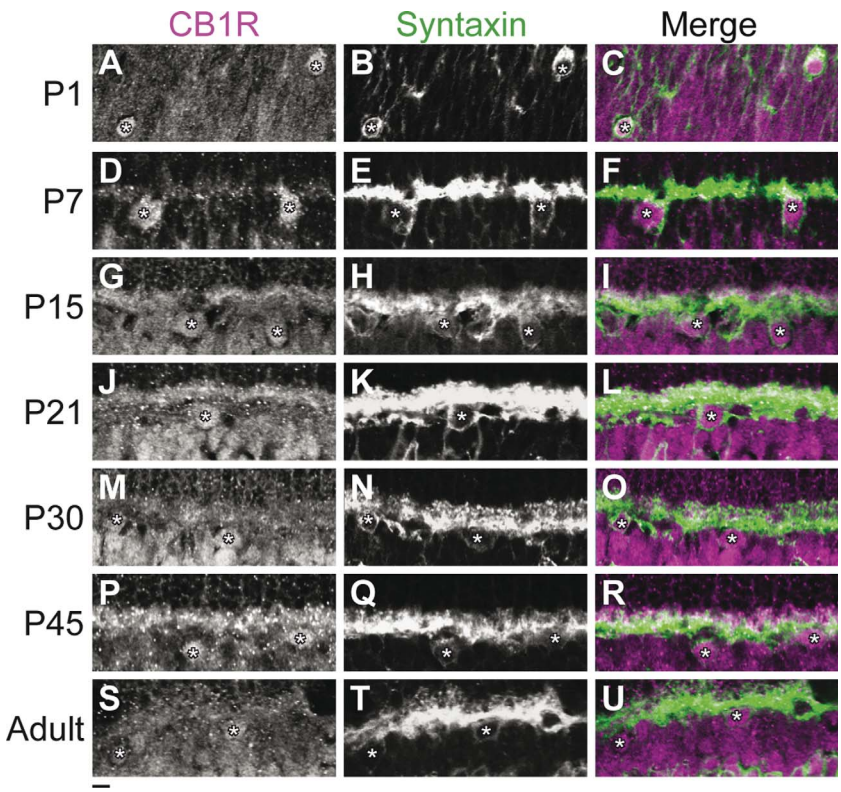

Figure 5. CB1R immunoreactivity in horizontal cells in the developing rat retina. **A–U:** Vertical sections from P1 (A–C), P7 (D–F), P15 (G–I), P21 (J–L), P30 (M–O), P45 (P–R), and adult (S–U) rat retinas. Confocal micrographs of retinas co-immunolabeled for CB1R and syntaxin, the cell-type-specific marker for the retinal interneurons (horizontal and amacrine cells). Each protein is presented alone in gray scale: CB1R in the first column and syntaxin in the second; then the two are presented merged (third column: CB1R in magenta and syntaxin in green). Horizontal somas are immunopositive for CB1R (stars) at all ages. Scale bar = 10 μm below S (applies to A–U).

amacrines cells, an additional 3D analysis was conducted at all ages. An example is shown in the adult in Figure 6U; no CB1R expression was visible along the three axes. These "transient-expressing" CB1R amacrine cells may represent a single population of cells that stopped expressing the receptor at P15 or several cells' populations that transiently ceased expressing CB1R at different time periods.

Ganglion cells expressed CB1R in their cell bodies throughout the entire time interval we studied. Examples of this expression are shown in Figure 7. As expected from previous studies (e.g., Perry et al., 1983; Galli-Resta and Ensini, 1996), a decrease in the number of ganglion cells with age was observed. Although there was no visible change in CB1R expression in the soma of ganglion cells, there was an increase of immunofluorescence in their axons between P1 and P15, after which expression remained stable (Fig. 3A–H). It is also worth mentioning that GCL cells other than RGCs were also immunopositive. These cells may be displaced amacrine cells.

Cones constitute the last class of early-born neurons to be generated in the retina (Rapaport et al., 2004). In these photoreceptors, CB1R was not expressed until P5 (Fig. 3A–C). Detailed pictures of CB1R expression in cones are presented in Figure 8A–N. Around P5, CB1R was present in the cell bodies (Fig. 8A) and pedicles (Fig. 8B). It can be seen that the cone pedicles made synapses onto horizontal cells (Fig. 8B). This neuronal contact was previously described by Rich et al. (1997) in their study on early cone development. At P11, the somas of cones were still CB1R immunopositive but were off-positioned compared with adults (Fig. 8C). A refinement of the cone pedicle, consistent with the completion of the cone-horizontal-bipolar triad, could be also appreciated at this stage (Fig. 8D). By P15, most cones have reached their final position in the ONL and they strongly expressed CB1R in all their cellular compartments (Fig. 8E,F). Over the following weeks, CB1R expression remained high in the outer and inner segments, cell body, axon, and pedicle of all cones throughout the period investigated (Fig. 8G–N).

Late-born neurons

During the first week of life, several developmental processes such as cell division, differentiation, and migration overlap. Late-born neurons are generated from neuroblasts, mostly in the 5–6 days following birth. They give

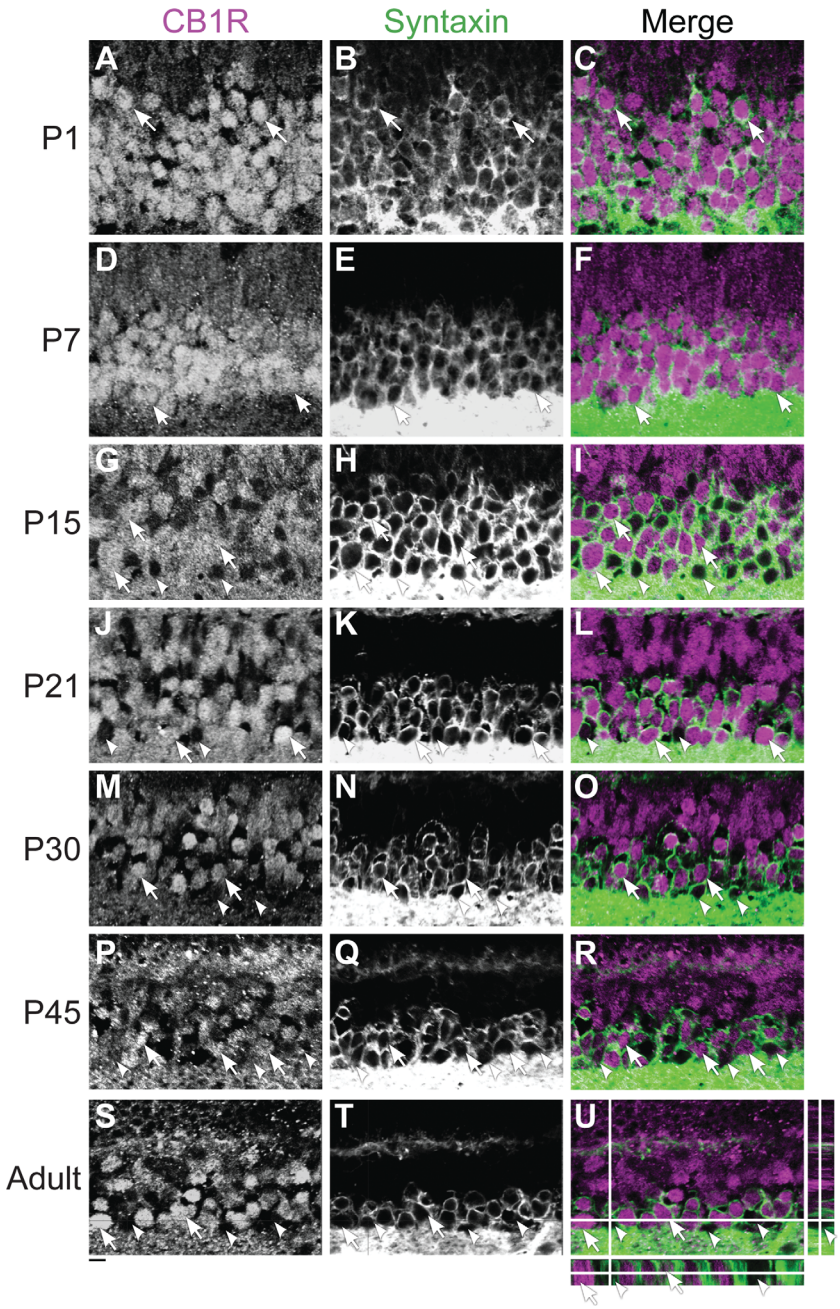

Figure 6. **A–U:** Vertical sections from P1 (A–C), P7 (D–F), P15 (G–I), P21 (J–L), P30 (M–O), P45 (P–R) and adult (S–U) rat retinas. Confocal micrographs of retinas co-immunolabeled for CB1R and syntaxin, the cell-type-specific marker for the retinal interneurons (horizontal and amacrine cells). Each protein is presented alone in gray scale: CB1R in the first column and syntaxin in the second; then the two are presented merged (third column: CB1R in magenta and syntaxin in green). CB1R-immunopositive and -immunonegative amacrine cells are indicated by arrows and arrowheads, respectively. In U, the horizontal and vertical insets show the reconstruction of the section in the X-Z and Y-Z plans, respectively, along the white lines. Scale bar = 10 μm below S (applies to A–U).

rise to bipolar cells, rod photoreceptors, and Müller cells (Morest, 1970; Rapaport et al., 2004).

At P1, the retina contained neuroblasts and dividing cells; the latter were identified by their morphology and position at the outer edge of the NBL (Baye and Link, 2007; Barton and Levine, 2008; and see Baye and Link, 2008 for review). Mitotic cells were CB1R positive, whereas neuroblasts were very lightly stained (Fig. 9A,B). The same pattern of expression was visible at P3, although the number of dividing cells was lower (Fig. 9C,D). At P5, there were only a few mitotic cells. Some of the neuroblasts located in the inner part of the emergent INL displayed an increase in CB1R immunofluorescence whereas those closer to the developing OPL did not

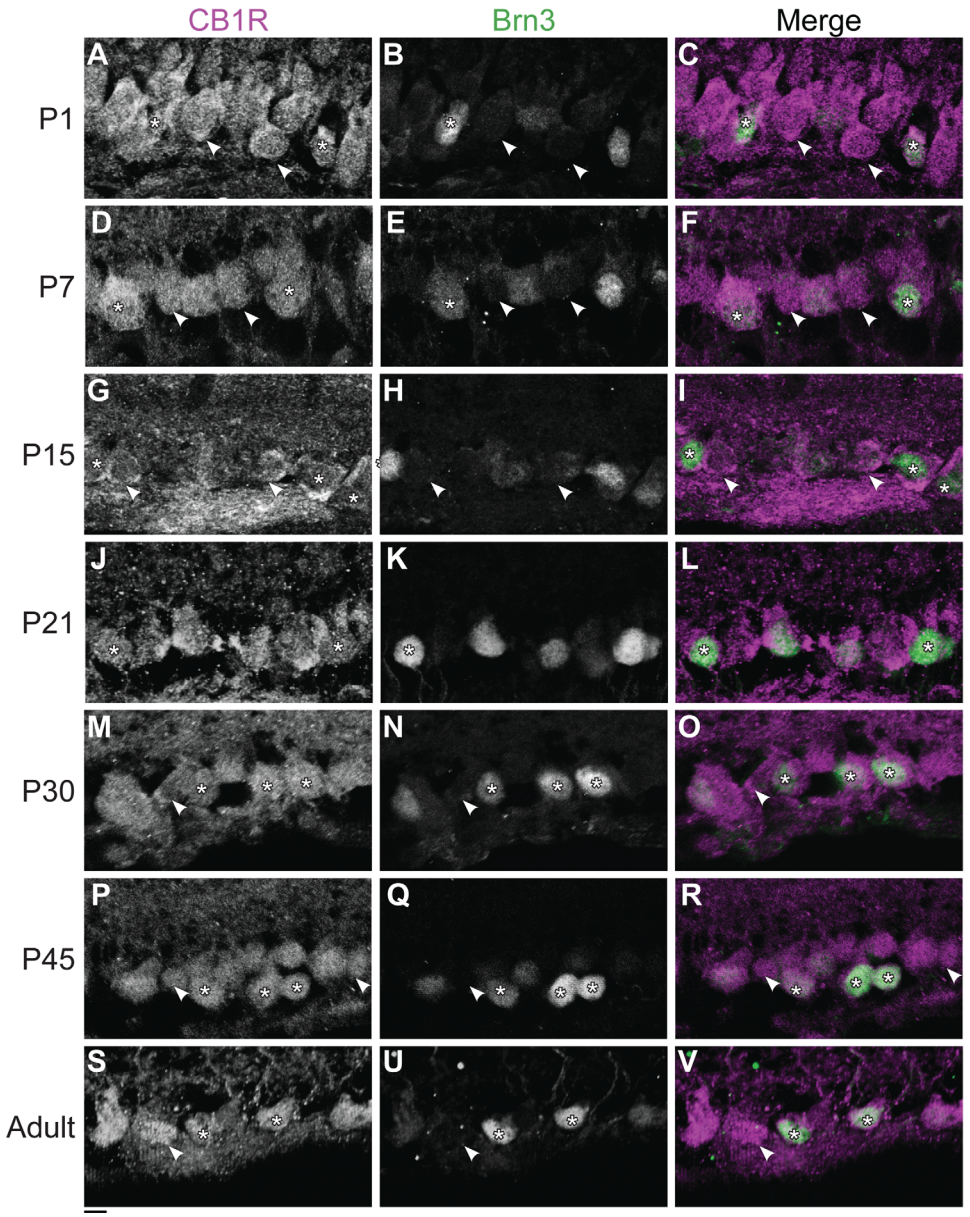

Figure 7. CB1R immunoreactivity in the ganglion cell layer in the developing rat retina. **A–V:** Vertical sections from P1 (A–C), P7 (D–F), P15 (G–I), P21 (J–L), P30 (M–O), P45 (P–R) and adult (S–V) rat retinas. Confocal micrographs of retinas co-immunolabeled for CB1R and the cell-type-specific marker for RGCs, Brn3. Each protein is presented alone in gray scale: CB1R in the first column and Brn3 in the second; then the two are presented merged (third column: CB1R in magenta and Brn3 in green). RGCs are immunopositive for CB1R (stars) at all ages. Other cells within the GCL (arrowheads), presumably displaced amacrine cells, are also immunopositive for CB1R across all ages. Scale bar = 10 μm below S (applies to A–V).

express the receptor (Fig. 9E,F). At P7, the few neuroblasts still present showed a light immunofluorescence for CB1R (Fig. 9G,H).

The expression of CB1R in rod bipolar cells is presented in Figure 10. Before P5, there were a few PKC-positive cells that could be either rod bipolar or amacrine cells. These cells could not always be told apart because most rod bipolar cells had not yet reached their final location. An example at P3, at which point they could be differentiated, is presented in Figure 10A–C. The cell identified by an arrowhead exhibited an immunofluorescence level comparable to that of the surrounding neuroblasts. Based on its location, the unit is likely a rod bipolar cell. In contrast, the cell identified by the arrow was strongly CB1R positive and, given its location and morphology, was considered to be an amacrine cell. Between P5 and P9, neurons in the INL closer to the IPL were CB1R positive, whereas those near the OPL were immunonegative (Fig. 10D–F). This upregulation of CB1R expression in the intermediate but not the most superficial part of the INL

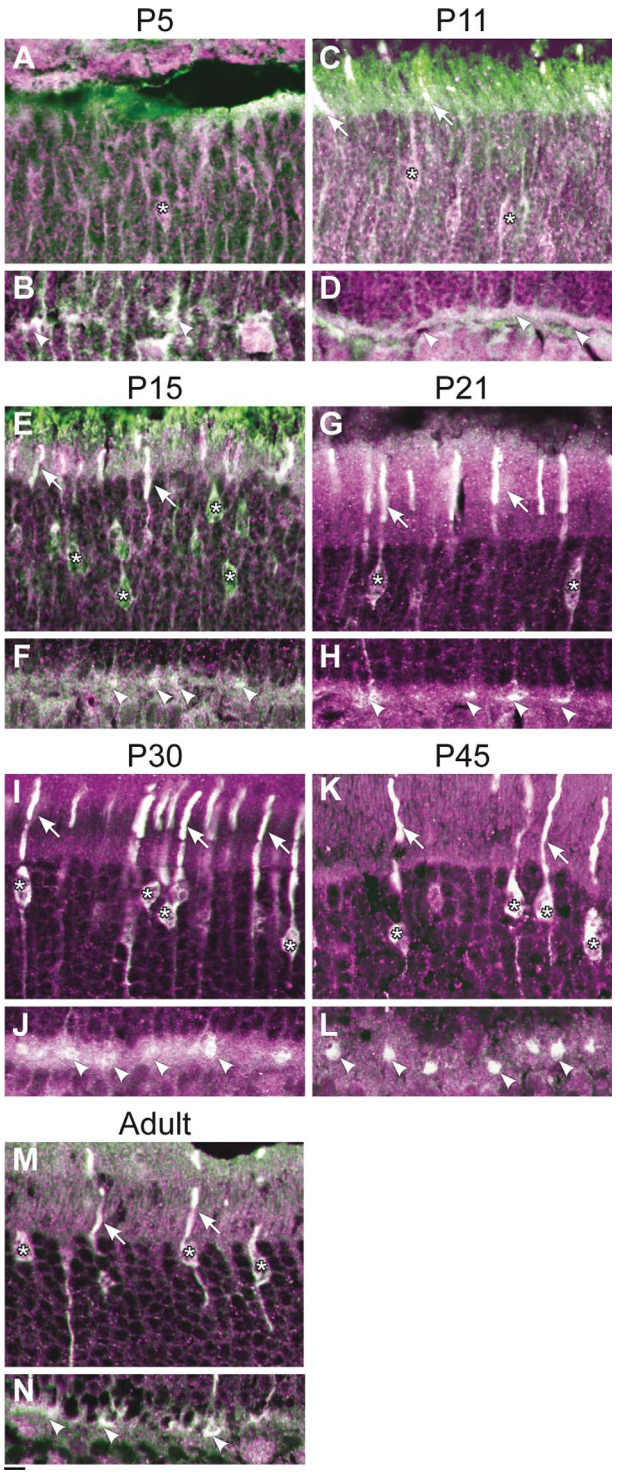

Figure 8. CB1R immunoreactivity in cone photoreceptors in the developing rat retina. **A–N:** Vertical sections from P5 (A,B), P11 (C,D), P15 (E,F), P21 (G,H), P30 (I,J), P45 (K,L), and adult (M.N) rat retinas. Confocal micrographs of retinas co-immunolabeled for CB1R (magenta) and the cell-type-specific marker for the cones, cone-transducin (green). Cones become immunopositive for CB1R at P5 and remain so throughout development and into adulthood. CB1R is expressed in the outer (arrow) and inner segments of the cone, as well as the cell body (stars), the axon, and the synaptic pedicle (arrowheads). Scale bar = 10 μm below N (applies to A–N).

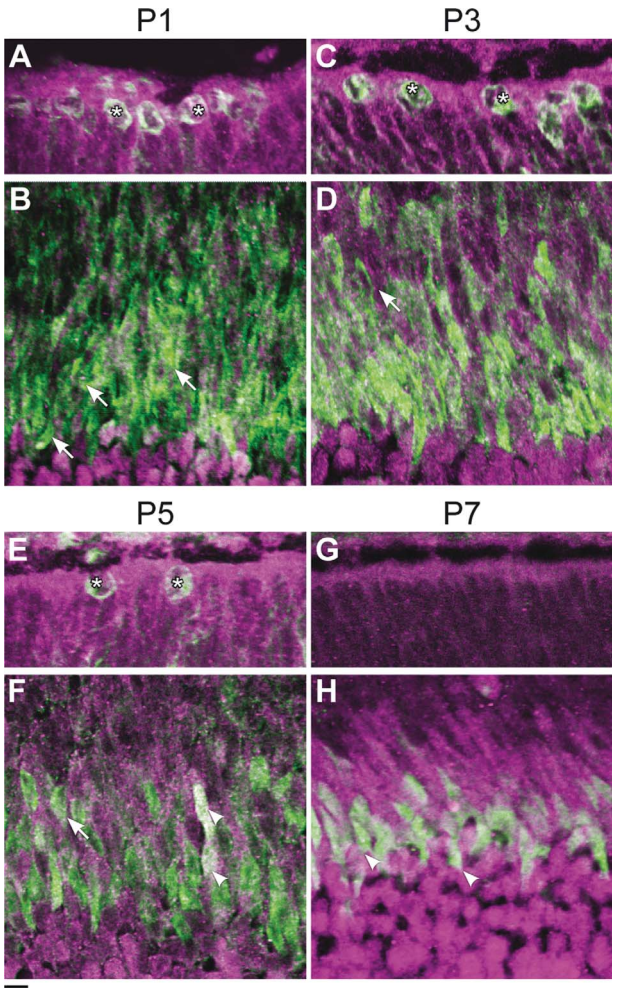

Figure 9. CB1R immunoreactivity in retinal progenitor (B,D,F,H) and mitotic cells (A,C,E,G) in the developing rat retina. **A–H:** Vertical sections from P1 (A,B), P3 (C,D), P5 (E,F), and P7 (G,H) rat retinas. Confocal micrographs of retinas co-immunolabeled for CB1R (magenta) and the cell-type-specific marker for the retinal progenitor and mitotic cells, PCNA (green). Mitotic cells (stars) are CB1R positive as long as they exist in the postnatal period, namely, until P5–6. Most neuroblasts are not CB1R positive (arrows). Some neuroblasts closer to the IPL are immunolabeled for CB1R (arrowsheads), and their number increases until they are all immunopositive for CB1R at P7. Scale bar = 10 μm below F (applies to A–H).

is consistent with the wave of expression described in Figure 3C and D at P5 and 7. During the second week of life (P15), CB1R labeling signal increased (Fig. 10G–I), yielding a diffuse and variable expression in the upper part of the INL across animals. By the end of the third week (P21; Fig. 10J–L), the CB1R expression in rod bipolar somas had decreased, and at P30 (Fig. 10M–O), no labeling of the cell body structure could be seen and only low and diffuse immunofluorescence was present. The latter could represent either some background noise or a weak signal.

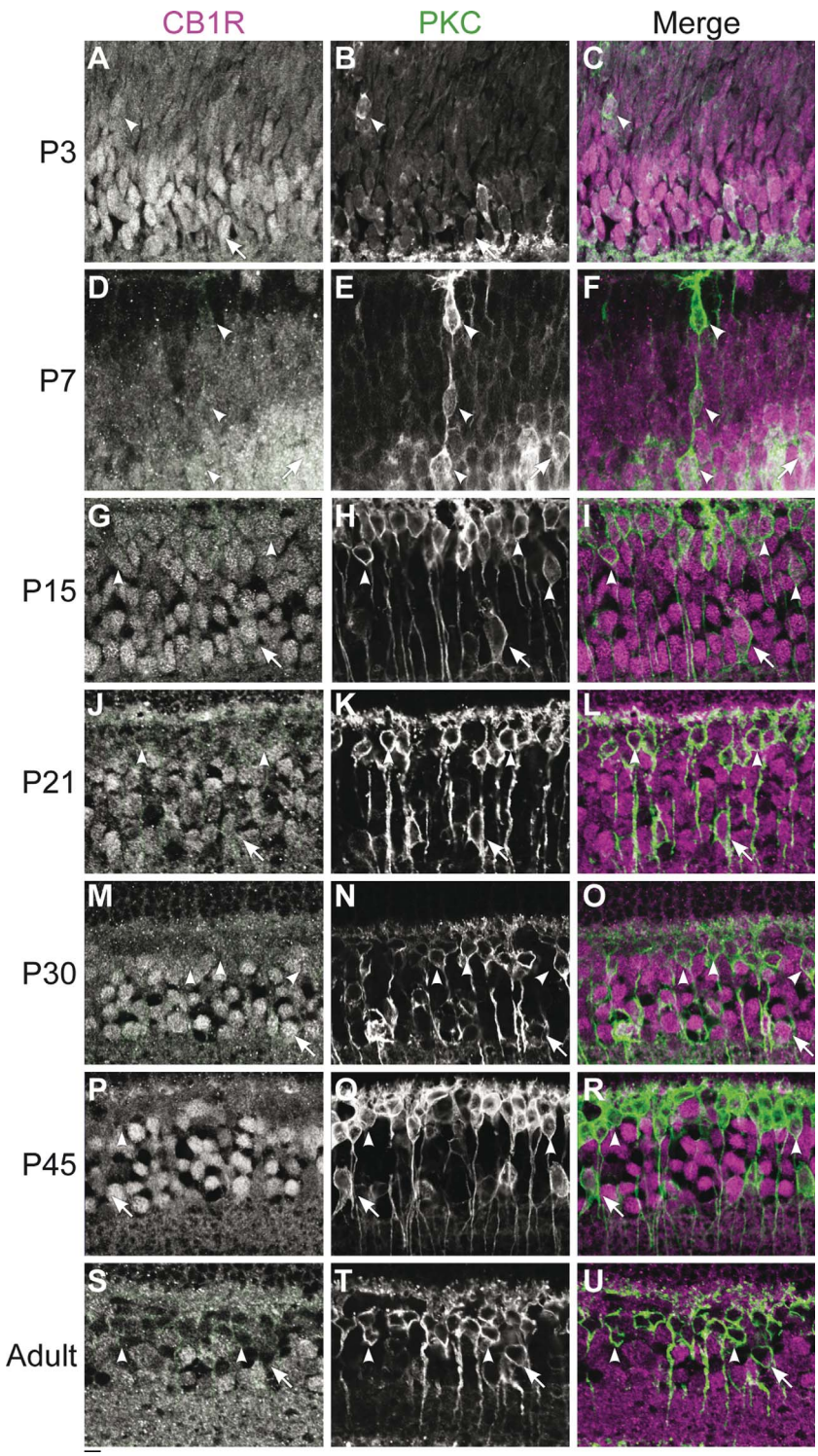

Figure 10. CB1R immunoreactivity in rod bipolar and some amacrine cells in the developing rat retina. **A–U:** Vertical sections from P3 (A–C), P7 (D–F), P15 (G–I), P21 (J–L), P30 (M–O), P45 (P–R) and adult (S–U) rat retinas. Confocal micrographs of retinas co-immunolabeled for CB1R and the cell-type-specific marker for the rod bipolar and a subtype of amacrine cells, PKCα. Each protein is presented alone in gray scale: CB1R in the first column and PKCα in the second; then the two are presented merged (third column: CB1R in magenta and PKCα in green). During their migration period, rod bipolar cells express CB1R when they are closer to the IPL (A,B, arrowheads) and become CB1R positive between P9 and P21 (C,D, arrowheads), after which they progressively lose CB1R labeling (E–G, arrowheads). PKCα-positive amacrine cells are CB1R immunolabeled throughout until P30 (A–E, arrows). Throughout the second month of life, CB1R appears to be more concentrated at the membrane of PKCα-positive amacrine cells (F,G, arrows). Scale bar = 10 μm below S (applies to (A–U).

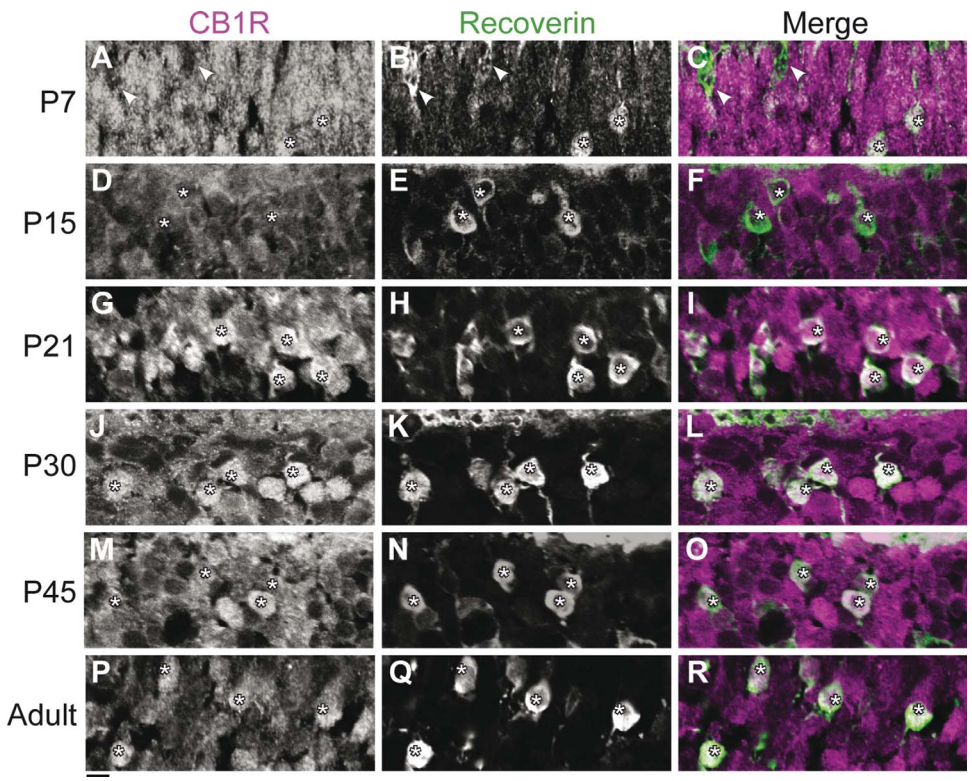

Figure 11. CB1R immunoreactivity in types 2 and 8 cone bipolar cells in the developing rat retina. **A–R:** Vertical sections from P7 (A–C), P15 (D–F), P21 (G–I), P30 (J–L), P45 (M–O), and adult (P–R) rat retinas. Confocal micrographs of retinas co-immunolabeled for CB1R and the cell-type-specific marker for types 2 and 8 of cone bipolar cells, recoverin. Each protein is presented alone in gray scale: CB1R in the first column and recoverin in the second; then the two are presented merged (third column: CB1R in magenta and recoverin in green). During their migration period, cone bipolar cells are not discernable prior to P7 with this marker. At P7, some cone bipolar cells express CB1R when they are closer to the IPL (stars in A–C), whereas some, closer to the OPL, do not (arrowhead in A–C). At older ages, all recoverin-positive bipolar cells are CB1R positive (stars). Scale bar = 10 μm below P (applies to A–R).

The fact that the CB1R antibody yielded almost no background in the knockout (KO) mice (Fig. 1A,B) suggests that the immunofluorescence probably came from CB1R expression in bipolar cells. At P45 and in adults (Fig. 10P–U), no receptor expression was visible in the somas, but some signal was detectable in the OPL at the level of the bipolar cells' dendrites. The white pixels were concentrated at the edges of the dendrites (Fig. 10R), and careful observation demonstrated that CB1R was outside the postsynaptic elements (i.e., bipolar cells).

CB1R expression in recoverin-positive bipolar cells was also investigated. Recoverin-positive bipolar cells are type 2 ON and type 8 OFF-cone bipolar cells (McGinnis et al., 1992a,b, 1997). These bipolar cells were not clearly discernable from rods until the OPL was formed, i.e., around P5–P7, as previously reported by Sharma et al. (2003). At P7, only a subpopulation of recoverin-positive cells in the INL was expressing CB1R (Fig. 11A–C). One can ask whether the bipolar cells that are not expressing CB1R are indeed lacking the receptor or are not yet expressing CB1R because they are still at an early developmental stage. The last suggestion seems more likely because all recoverin-positive bipolar cells at P21, P30, P45, and in adults express CB1R (Fig. 11D–R).

Rods constitute the vast majority of photoreceptors in the rat's retina. We showed in Figure 3 that only a few photoreceptors were CB1R positive and suggested that these cells were cones. This was verified by using a cone-specific marker. Only these cone-transducin-labeled cells expressed CB1R (Fig. 7). These data indicate that rods do not express CB1R at any age.

Müller cells are generated late in development and begin to express GS around P5 (Riepe and Norenberg, 1978). Müller cells were clearly distinguishable at P5 and already expressed CB1R in their cell bodies and processes (from P5 to P9; see example at P7 in Fig. 12A–C). From P9, CB1R was downregulated in these cells (see the weak immunofluorescence at P15; Fig. 12D–F), and its expression could not be distinguished from background at and after P21 (Fig. 12G–R).

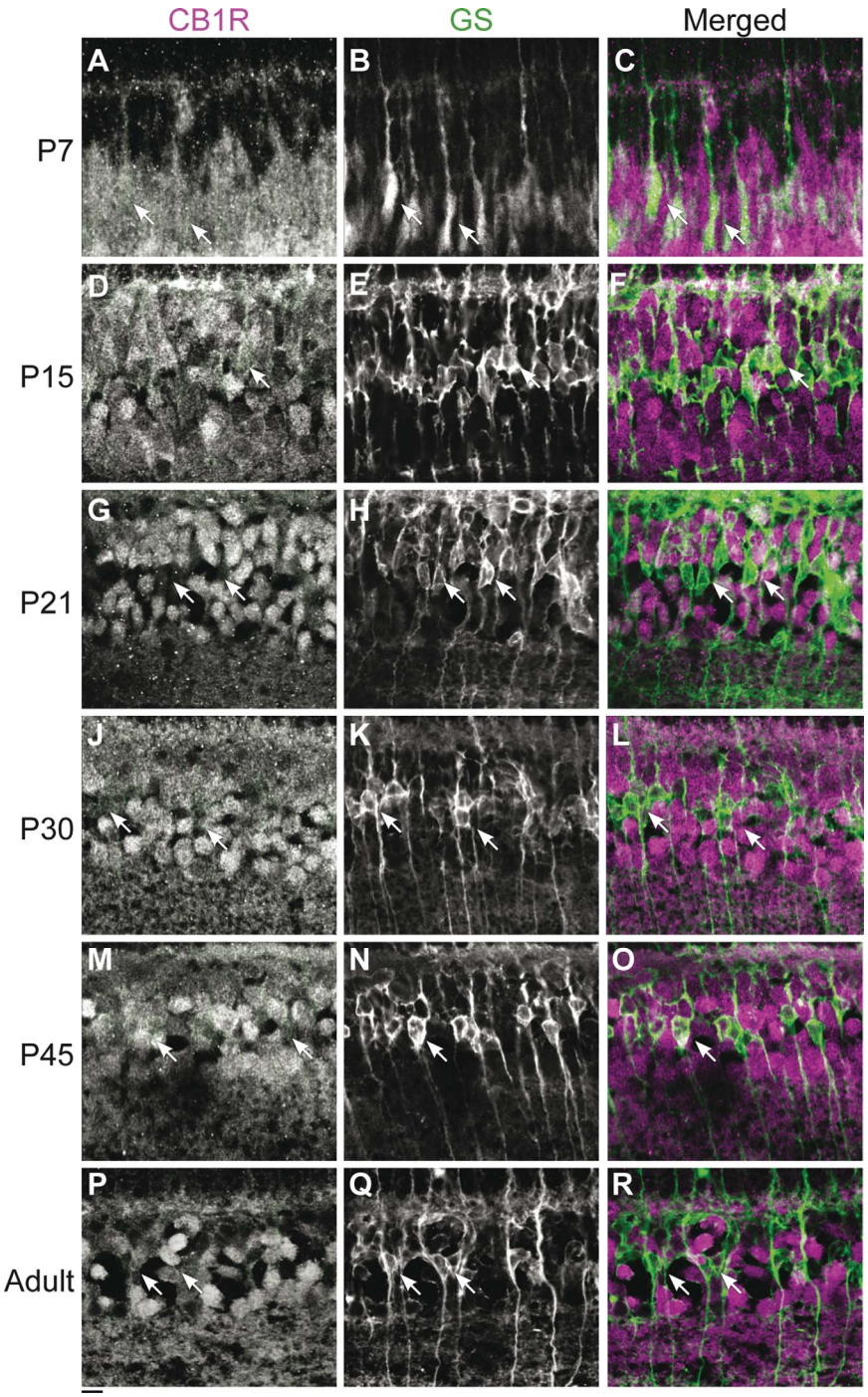

Figure 12. CB1R immunoreactivity in Müller cells in the developing rat retina. **A–R:** Vertical sections from P7 (A–C), P15 (D–F), P21 (G–I), P30 (J–L), P45 (M–O), and adult (P–R) rat retinas. Confocal micrographs of retinas co-immunolabeled for CB1R and the cell-type-specific marker for glial Müller cells, glutamine synthetase (GS). Each protein is presented alone in gray scale: CB1R in the first column and GS in the second; then the two are presented merged (third column: CB1R in magenta and GS in green). This marker becomes visible in Müller cells around P5 and is well discernable at P7. At P7 Müller cells express CB1R (A–C, arrows), but they become CB1R negative at older ages (P21–adult; arrows). Scale bar = 10 μm below P (applies to A–R).

DISCUSSION

This study is the first to investigate the postnatal development of CB1R expression in the main cell types of the rodent retina. By using immunohistological staining and immunoblots, we demonstrated that both the localization and total amount of CB1R vary during postnatal development and maturation of the retina of Long-Evans rats. Our data showed evidence of an early and widespread

expression of CB1R, i.e., most cell types expressed the receptor, either transiently or permanently. Starting at P1, CB1R was expressed by all early-born neurons, except cones. As development occurred, CB1 receptors appeared in cone photoreceptors and bipolar cells. Rod bipolar cells displayed a transient expression of CB1R between P5 and P21, whereas recoverin-positive cone bipolar cells started expressing CB1R around the end of the first week of life and remained CB1R positive into adulthood. Overall, these data, and particularly the transient nature of CB1R expression in some cell types, suggest that the endocannabinoid system is involved in developmental and/or maturational processes.

Temporal expression of the endocannabinoid system

As expected, retinal immunoblots revealed a CB1R band at around 53 kDa, consistent with its nonglycosylated monomer form reported in rodent and human retinal tissues (Yazulla et al., 1999; Porcella et al., 2000). In the present study, we observed that CB1R expression was age dependent, going from a lower to a higher concentration between the second and third weeks of life. An increase in concentration of the receptor during development has also been reported in brain structures such as the striatum (Rodriguez de Fonseca et al., 1993), hippocampus (Berrendero et al., 1999), cerebellum (McLaughlin and Abood, 1993; Belue et al., 1995; Berrendero et al., 1999), and cerebral cortex (Berrendero et al., 1999). Our data are in agreement with these studies, indicating an upregulation of CB1R expression in the rodent CNS during postnatal development.

In contrast to classical neurotransmitters, endocannabinoids, being lipophilic compounds, are not stored in vesicles. They are rather produced locally at the moment of their intended action. This model indicates that both biosynthetic and degradative enzymes are key regulators of lipid signaling. The level of endogenous CB1R ligand depends on both the activity and genetic expression of these enzymes. We investigated one aspect of this equation by studying the temporal expression of the biosynthetic and degradative enzymes. NAPE-PLD, DAGLα, and FAAH bands were found at around 46 kDa, 120 kDa, and 66 kDa, respectively, in agreement with previous observations in other structures in the CNS (Cravatt et al., 1996; Egertova et al., 1998; Yazulla et al., 1999; Cravatt et al., 2001; Okamoto et al., 2004; Rimmerman et al., 2008). Our data demonstrated that the expression of FAAH decreased during the first week of life, whereas the expression of NAPE-PLD and DAGLα remained stable, suggesting that the concentration of endocannabinoids increased over this period. This possibility is supported by the fact that AEA level increases during postnatal development in brain areas (Berrendero et al., 1999; Ade and Lovinger, 2007). During the second week of life, FAAH increased, whereas both synthetic enzymes remained stable, suggestive of a reduction in endocannabinoid concentration. The age dependency of NAPE-PLD and FAAH expression was also observed in brain areas (Thomas et al., 1997; Morishita et al., 2005), albeit the temporal pattern of expression in these structures differed from the one we observed in the retina (e.g., steady increase until P30 for NAPE-PLD and until P10 for FAAH).

CB1R expression during retinal development

The various phases of retinal postnatal development in mice and rats have been previously described in much detail by several groups, using immunohistochemical and cell dating techniques (Fletcher and Kalloniatis, 1997; Sharma et al., 2003; Rapaport et al., 2004). The chronology of the postnatal events observed here is in total agreement with the above-mentioned studies. Briefly, at birth the retina is comprised of the NBL (which contains undifferentiated neuroblasts, immature cones, interneurons, i.e., horizontal and amacrine cells, and a few rods), the IPL, and the ganglion cell layer (which also includes displaced amacrine cells). During the first week of life, bipolar, Müller cells and rods are generated (Fletcher and Kalloniatis, 1997; Sharma et al., 2003; Rapaport et al., 2004). During the same time interval, early-born neurons continue to mature; one example would be cone photoreceptors, which establish synaptic contacts with horizontal cells by P5 and complete the cone-horizontal-bipolar triad by P10 (this study; Rich et al., 1997; Hack et al., 2002).

RGCs and amacrine cells

CB1R was expressed in most early-born neurons as early as P1. This is in line with other studies that revealed the presence of CB1R mRNA in RGCs at E15 in rats (Buckley et al., 1998) and at E18 in chicks (Begbie et al., 2004). CB1R immunofluorescence remained constant in the soma of RGCs from P1 to P15, but increased in RGCs axons in the nerve fiber layer during the same period (data not shown). This is consistent with the presence of CB1R along the retinothalamic pathway during postnatal development (Argaw et al., 2008) and the contribution of endocannabinoids in RCG growth cone navigation and proper targeting, both in vivo and in vitro (Argaw et al., 2009).

CB1R expression stayed constant in most amacrine cells throughout development. For the remaining cells, it was transiently expressed (CB1R-negative amacrine cells appearing around P15), suggesting that, for these units, CB1R expression is only related to developmental

processes (see the section on functional considerations below).

Cones and horizontal cells

CB1R was present in horizontal cells as early as P1 and remained stable throughout the entire postnatal development and into adulthood. CB1R appeared later in cones (around P5), in their cell bodies and pedicles. These findings are in agreement with previous observations made in adult animals. For instance, the presence of CB1R in horizontal cells was demonstrated in the retina of adult albino rats by Yazulla et al. (1999). The receptor's expression in cone terminals was reported in a number of species, i.e., chick (Leonelli et al., 2005), goldfish (Struik et al., 2006), salamander (Straiker and Sullivan, 2003), rat (Straiker et al., 1999; Yazulla et al., 1999), mouse (Straiker et al., 1999; Yazulla, 2008), and monkey (Straiker et al., 1999). Thus, the presence of CB1R in cone pedicles across species suggests that the contribution of this receptor in cone functioning was conserved during evolution. Given the role of CB1R in retrograde signaling (see for review Kreitzer and Regehr, 2002), its appearance in cone synapses at P5, i.e., 5 days prior to the emergence of the postsynaptic component of the cone-horizontal-bipolar triad (Rich et al., 1997; Hack et al., 2002), is rather intriguing. However, the timing of CB1R expression coincides with the appearance of the first cone-horizontal cells synapses in the forming OPL (Rich et al, 1997; Dhingra et al., 1997; Hack et al., 2002). Thus, the receptor may be necessary to refine synaptic connections between these two cell types.

In support of this assumption, cone photoreceptors are known to modulate the organization of horizontal cell dendritic trees through early glutamatergic activation (starting around P2; Raven et al., 2008). Also, endocannabinoids synthesis is known to be activity dependent (see Freund et al., 2003 for review), and CB1R was shown to negatively modulate glutamatergic release from cones in goldfish retina through retrograde signaling (Fan and Yazulla, 2007). The synaptic refinement can also originate from horizontal cells. Around P5, these cells transiently contain GABA (Schnitzer and Rusoff, 1984; Fletcher and Kalloniatis, 1997), and its release was shown to be modulated by CB1R in embryonic retinal interneurons (Warrier and Wilson, 2007). Moreover, GABA release from horizontal cells can modulate cone photoreceptor synaptogenesis in rabbits (Fletcher and Kalloniatis, 1997; Mitchell et al., 1999) and cone mosaic organization in mice (Fei, 2003). These cumulative data place CB1R in a strategic position to modulate synaptogenesis of both cones and horizontal cells, a role demonstrated in the hippocampus by Kim and Thayer (2001). The role of CB1R may not be limited to synaptogenesis. It has been shown that cones are displaced and migrate back to their position between P4 and 12 (Rich et al., 1997). CB1R may be involved in this process as well because it can influence cell migration (Song and Zhong, 2000; Berghuis et al., 2007; Mulder et al., 2008).

CB1R expression in late-born cells

All groups of late-born cells, except rods, expressed CB1R around P5–P9, a period that corresponds to developmental processes such as cell migration, subtype identity acquisition, and morphological changes (Sharma et al., 2003; Bramblett et al., 2004; Morgan et al., 2006; Schroeter et al., 2006). However, not all cells in each group were labeled. Neuroblasts expressed CB1R relatively late (around P5), and only cells closer to the IPL were labeled. The other neuroblasts did not express CB1R. Likewise, recoverin- and PKC-positive bipolar cells closer to the IPL were immunopositive around P7, whereas those closer to the OPL did not express CB1R. CB1R was transiently expressed in Müller cells during cell migration (P5–P7). These observations suggest that this receptor is likely involved in the cell migration and morphological changes of rod bipolar and Müller cells. A similar statement can be made for cone bipolar cells, but in this case CB1R could also be involved in subtype identity acquisition. A contribution of CB1R in these developmental stages has been reported in the hippocampus and in cultured cortical neurons (Gomez et al., 2003, 2007, 2008a,b; Harkany et al., 2008; Mulder et al., 2008).

It should be noted that CB1R expression in rod bipolar cells was difficult to analyze in late postnatal development (after P15) because it became diffuse and variable. A previous study (Straiker et al., 1999) also reported difficulty in identifying the presence of CB1R expression in this cell type using immunohistochemical techniques. These authors were, however, able to demonstrate its presence with electrophysiological techniques. This could indicate that, in this cell type, CB1R antigenicity is highly sensitive to fixation process. Given that the antibodies used in this study and in Straiker et al. (1999) were raised against the same portion of the protein (amino acids 1–77), another possible explanation would be that CB1R adopts a conformation that makes the epitope less accessible to these antibodies.

Functional considerations

During the first week of life, spontaneous activity could be an important mechanism by which visual map refinement occurs in thalamic nuclei (McLaughlin et al., 2003; Syed et al., 2004; Torborg and Feller, 2005; Zheng et al., 2006). Spontaneous discharges have been shown to originate from amacrine and ganglion cells (Masland et al., 1984; Tauchi and Masland, 1984; Feller et al., 1996;

Zhou, 1998; Bansal et al., 2000; Sernagor et al., 2000; Wong et al., 2000; Zhou and Zhao, 2000; Stacy et al., 2005; Zheng et al., 2006), two cell types expressing CB1R during the first week of life. Given that both endocannabinoid synthesis and function are modulated by neural activity (see for review Freund et al., 2003), one can propose that a propagating wave of spontaneous activity could cause local changes in endocannabinoid concentration, which would in turn limit the spread of spontaneous activity through CB1R activation. This could be mediated by amacrine cells given that these cells negatively modulate spontaneous retinal waves (Wang et al., 2007) and that the endocannabinoid system modulates spontaneous neurotransmitter release in embryonic GABAergic amacrine cell cultures (Warrier and Wilson, 2007).

The proposal that endocannabinoids can modulate spontaneous activity, and therefore be involved in the establishment (or refinement) of topographic maps, would be in line with the findings of two previous studies. In the first, the exogenous activation of endocannabinoid signaling in the developing hippocampus caused an abnormal shutdown of neural activity, whereas its downregulation yielded epileptic activity (Bernard et al., 2005). In the second study, the abnormal activation of CB1R during the critical period caused abnormal maps in the somatosensory cortex in rodents (Li et al., 2009). Altogether, these studies, including ours, place the endocannabinoid system in a strategic position to negatively modulate retinal patterned activity and support the notion that CB1R could be important for the normal organization of visual thalamic nuclei afferents.

ACKNOWLEDGMENTS

We are grateful to Beat Lutz for providing the *CB1R* transgenic tissue and to Denis Boire for comments on a draft of the manuscript. We also thank Michel Cayouette for his assistance in the choice of the antibodies.

LITERATURE CITED

Acosta ML, Bumsted O'Brien KM, Tan SS, Kalloniatis M. 2008. Emergence of cellular markers and functional ionotropic glutamate receptors on tangentially dispersed cells in the developing mouse retina. J Comp Neurol 506:506–523.

Ade KK, Lovinger DM. 2007. Anandamide regulates postnatal development of long-term synaptic plasticity in the rat dorsolateral striatum. J Neurosci 27:2403–2409.

Aguado T, Monory K, Palazuelos J, Stella N, Cravatt B, Lutz B, Marsicano G, Kokaia Z, Guzman M, Galve-Roperh I. 2005. The endocannabinoid system drives neural progenitor proliferation. FASEB J 19:1704–1706.

Argaw A, Duff G, Ptito M, Bouchard J-F. 2008. Contribution of the endocannabinoid CB1 receptor during axon guidance Program No. 624.1/B38. Neuroscience (2008) Abstracts. Washigton, DC: Society for Neuroscience. Online.

Argaw A, Duff G, Tea N, Ptito M, Bouchard J-F. 2009. The endocannabinoid system modulates axon guidance and target selection during development. Program No. 129.8/B29. Neuroscience (2009) Abstracts. Chicago, IL: Society for Neuroscience.

Bansal A, Singer JH, Hwang BJ, Xu W, Beaudet A, Feller MB. 2000. Mice lacking specific nicotinic acetylcholine receptor subunits exhibit dramatically altered spontaneous activity patterns and reveal a limited role for retinal waves in forming ON and OFF circuits in the inner retina. J Neurosci 20:7672–7681.

Barker PA, Shooter EM. 1994. Disruption of NGF binding to the low affinity neurotrophin receptor p75LNTR reduces NGF binding to TrkA on PC12 cells. Neuron 13:203–215.

Barnstable CJ, Hofstein R, Akagawa K. 1985. A marker of early amacrine cell development in rat retina. Brain Res 352:286–290.

Barton KM, Levine EM. 2008. Expression patterns and cell cycle profiles of PCNA, MCM6, cyclin D1, cyclin A2, cyclin B1, and phosphorylated histone H3 in the developing mouse retina. Dev Dyn 237:672–682.

Baye LM, Link BA. 2007. Interkinetic nuclear migration and the selection of neurogenic cell divisions during vertebrate retinogenesis. J Neurosci 27:10143–10152.

Baye LM, Link BA. 2008. Nuclear migration during retinal development. Brain Res 1192:29–36.

Begbie J, Doherty P, Graham A. 2004. Cannabinoid receptor, CB1, expression follows neuronal differentiation in the early chick embryo. J Anat 205:213–218.

Belue RC, Howlett AC, Westlake TM, Hutchings DE. 1995. The ontogeny of cannabinoid receptors in the brain of postnatal and aging rats. Neurotoxicol Teratol 17:25–30.

Berghuis P, Dobszay MB, Wang X, Spano S, Ledda F, Sousa KM, Schulte G, Ernfors P, Mackie K, Paratcha G, Hurd YL, Harkany T. 2005. Endocannabinoids regulate interneuron migration and morphogenesis by transactivating the TrkB receptor. Proc Natl Acad Sci U S A 102:19115–19120.

Berghuis P, Rajnicek AM, Morozov YM, Ross RA, Mulder J, Urban GM, Monory K, Marsicano G, Matteoli M, Canty A, Irving AJ, Katona I, Yanagawa Y, Rakic P, Lutz B, Mackie K, Harkany T. 2007. Hardwiring the brain: endocannabinoids shape neuronal connectivity. Science 316:1212–1216.

Bernard C, Milh M, Morozov YM, Ben-Ari Y, Freund TF, Gozlan H. 2005. Altering cannabinoid signaling during development disrupts neuronal activity. Proc Natl Acad Sci U S A 102:9388–9393.

Berrendero F, Sepe N, Ramos JA, Di Marzo V, Fernandez-Ruiz JJ. 1999. Analysis of cannabinoid receptor binding and mRNA expression and endogenous cannabinoid contents in the developing rat brain during late gestation and early postnatal period. Synapse 33:181–191.

Bramblett DE, Pennesi ME, Wu SM, Tsai MJ. 2004. The transcription factor Bhlhb4 is required for rod bipolar cell maturation. Neuron 43:779–793.

Brandon C. 1985. Improved immunocytochemical staining through the use of Fab fragments of primary antibody, Fab-specific second antibody, and Fab-horseradish peroxidase. J Histochem Cytochem 33:715–719.

Buckley NE, Hansson S, Harta G, Mezey E. 1998. Expression of the CB1 and CB2 receptor messenger RNAs during embryonic development in the rat. Neuroscience 82:1131–1149.

Chang ML, Wu CH, Jiang-Shieh YF, Shieh JY, Wen CY. 2007. Reactive changes of retinal astrocytes and Muller glial cells in kainate-induced neuroexcitotoxicity. J Anat 210:54–65.

Cinar O, Semiz O, Can A. 2006. A microscopic survey on the efficiency of well-known routine chemical fixatives on cryosections. Acta Histochem 108:487–496.

Coleman JE, Zhang Y, Brown GA, Semple-Rowland SL. 2004. Cone cell survival and downregulation of GCAP1 protein in the retinas of GC1 knockout mice. Invest Ophthalmol Vis Sci 45:3397–3403.

Cravatt BF, Giang DK, Mayfield SP, Boger DL, Lerner RA, Gilula NB. 1996. Molecular characterization of an enzyme that degrades neuromodulatory fatty-acid amides. Nature 384:83–87.

Cravatt BF, Demarest K, Patricelli MP, Bracey MH, Giang DK, Martin BR, Lichtman AH. 2001. Supersensitivity to anandamide and enhanced endogenous cannabinoid signaling in mice lacking fatty acid amide hydrolase. Proc Natl Acad Sci U S A 98:9371–9376.

Deutsch DG, Chin SA. 1993. Enzymatic synthesis and degradation of anandamide, a cannabinoid receptor agonist. Biochem Pharmacol 46:791–796.

Dhingra NK, Ramamohan Y, Raju TR. 1997. Developmental expression of synaptophysin, synapsin I and syntaxin in the rat retina. Brain Res Dev Brain Res 102:267–273.

Egertova M, Giang DK, Cravatt BF, Elphick MR. 1998. A new perspective on cannabinoid signalling: complementary localization of fatty acid amide hydrolase and the CB1 receptor in rat brain. Proc Biol Sci 265:2081–2085.

Elshatory Y, Deng M, Xie X, Gan L. 2007. Expression of the LIM-homeodomain protein Isl1 in the developing and mature mouse retina. J Comp Neurol 503:182–197.

Fan SF, Yazulla S. 2003. Biphasic modulation of voltage-dependent currents of retinal cones by cannabinoid CB1 receptor agonist WIN 55212-2. Vis Neurosci 20:177–188.

Fan SF, Yazulla S. 2007. Retrograde endocannabinoid inhibition of goldfish retinal cones is mediated by 2-arachidonoyl glycerol. Vis Neurosci 24:257–267.

Fei Y. 2003. Development of the cone photoreceptor mosaic in the mouse retina revealed by fluorescent cones in transgenic mice. Mol Vis 9:31–42.

Feller MB, Wellis DP, Stellwagen D, Werblin FS, Shatz CJ. 1996. Requirement for cholinergic synaptic transmission in the propagation of spontaneous retinal waves. Science 272:1182–1187.

Fletcher EL, Kalloniatis M. 1997. Localisation of amino acid neurotransmitters during postnatal development of the rat retina. J Comp Neurol 380:449–471.

Freund TF, Katona I, Piomelli D. 2003. Role of endogenous cannabinoids in synaptic signaling. Physiol Rev 83:1017–1066.

Fride E. 2008. Multiple roles for the endocannabinoid system during the earliest stages of life: pre- and postnatal development. J Neuroendocrinol 20(suppl 1):75–81.

Galli-Resta L, Ensini M. 1996. An intrinsic time limit between genesis and death of individual neurons in the developing retinal ganglion cell layer. J Neurosci 16:2318–2324.

Gaillard F, Bonfield S, Gilmour GS, Kuny S, Mema SC, Martin BT, Smale L, Crowder N, Stell WK, Sauve Y. 2008. Retinal anatomy and visual performance in a diurnal cone-rich laboratory rodent, the Nile grass rat (*Arvicanthis niloticus*). J Comp Neurol 510:525–538.

Galve-Roperh I, Aguado T, Rueda D, Velasco G, Guzman M. 2006. Endocannabinoids: a new family of lipid mediators involved in the regulation of neural cell development. Curr Pharm Des 12:2319–2325.

Gao Y, Vasilyev DV, Goncalves MB, Howell FV, Hobbs C, Reisenberg M, Shen R, Zhang MY, Strassle BW, Lu P, Mark L, Piesla MJ, Deng K, Kouranova EV, Ring RH, Whiteside GT, Bates B, Walsh FS, Williams G, Pangalos MN, Samad TA, Doherty P. 2010. Loss of retrograde endocannabinoid signaling and reduced adult neurogenesis in diacylglycerol lipase knock-out mice. J Neurosci 30:2017–2024.

Gargini C, Terzibasi E, Mazzoni F, Strettoi E. 2007. Retinal organization in the retinal degeneration 10 (rd10) mutant mouse: a morphological and ERG study. J Comp Neurol 500:222–238.

Ghosh KK, Bujan S, Haverkamp S, Feigenspan A, Wassle H. 2004. Types of bipolar cells in the mouse retina. J Comp Neurol 469:70–82.

Gomez M, Hernandez M, Johansson B, de Miguel R, Ramos JA, Fernandez-Ruiz J. 2003. Prenatal cannabinoid and gene expression for neural adhesion molecule L1 in the fetal rat brain. Brain Res Dev Brain Res 147:201–207.

Gomez M, Hernandez M, Fernandez-Ruiz J. 2007. The activation of cannabinoid receptors during early postnatal development reduces the expression of cell adhesion molecule L1 in the rat brain. Brain Res 1145:48–55.

Gomez M, Hernandez M, Fernandez-Ruiz J. 2008a. Cannabinoid signaling system: does it play a function in cell proliferation and migration, neuritic elongation and guidance and synaptogenesis during brain ontogenesis? Cell Adh Migr 2:246–248.

Gomez M, Hernandez ML, Pazos MR, Tolon RM, Romero J, Fernandez-Ruiz J. 2008b. Colocalization of CB1 receptors with L1 and GAP-43 in forebrain white matter regions during fetal rat brain development: evidence for a role of these receptors in axonal growth and guidance. Neuroscience 153:687–699.

Goldenthal KL, Hedman K, Chen JW, August JT, Willingham MC. 1985. Postfixation detergent treatment for immunofluorescence suppresses localization of some integral membrane proteins. J Histochem Cytochem 33:813–820.

Hack I, Koulen P, Peichl L, Brandstatter JH. 2002. Development of glutamatergic synapses in the rat retina: the postnatal expression of ionotropic glutamate receptor subunits. Vis Neurosci 19:1–13.

Haque ME, Thomas KJ, D'Souza C, Callaghan S, Kitada T, Slack RS, Fraser P, Cookson MR, Tandon A, Park DS. 2008. Cytoplasmic Pink1 activity protects neurons from dopaminergic neurotoxin MPTP. Proc Natl Acad Sci U S A 105:1716–1721.

Harkany T, Keimpema E, Barabas K, Mulder J. 2008. Endocannabinoid functions controlling neuronal specification during brain development. Mol Cell Endocrinol 286(suppl 1): S84–90.

Haverkamp S, Wässle H. 2000. Immunocytochemical analysis of the mouse retina. J Comp Neurol 424:1–23.

Haverkamp S, Ghosh KK, Hirano AA, Wässle H. 2003. Immunocytochemical description of five bipolar cell types of the mouse retina. J Comp Neurol 455(4):463–476.

Herkenham M. 1991. Characterization and localization of cannabinoid receptors in brain: an in vitro technique using slide-mounted tissue sections. NIDA Res Monogr 112: 129–145.

Hill MN, Kambo JS, Sun JC, Gorzalka BB, Galea LA. 2006. Endocannabinoids modulate stress-induced suppression of hippocampal cell proliferation and activation of defensive behaviours. Eur J Neurosci 24:1845–1849.

Hirano AA, Brandstatter JH, Brecha NC. 2005. Cellular distribution and subcellular localization of molecular components of vesicular transmitter release in horizontal cells of rabbit retina. J Comp Neurol 488:70–81.

Hojo M, Ohtsuka T, Hashimoto N, Gradwohl G, Guillemot F, Kageyama R. 2000. Glial cell fate specification modulated by the bHLH gene Hes5 in mouse retina. Development 127:2515–2522.

Ino H, Chiba T. 2000. Expression of proliferating cell nuclear antigen (PCNA) in the adult and developing mouse nervous system. Brain Res Mol Brain Res 78:163–174.

Inoue A, Obata K, Akagawa K. 1992. Cloning and sequence analysis of cDNA for a neuronal cell membrane antigen, HPC-1. J Biol Chem 267:10613–10619.

Johnson PT, Williams RR, Reese BE. 2001. Developmental patterns of protein expression in photoreceptors implicate distinct environmental versus cell-intrinsic mechanisms. Vis Neurosci 18:157–168.

Kanda A, Swaroop A. 2009. A comprehensive analysis of sequence variants and putative disease-causing mutations in photoreceptor-specific nuclear receptor NR2E3. Mol Vis 15:2174–2184.

Kim D, Thayer SA. 2001. Cannabinoids inhibit the formation of new synapses between hippocampal neurons in culture. J Neurosci 21:RC146.

Kim DS, Ross SE, Trimarchi JM, Aach J, Greenberg ME, Cepko CL. 2008. Identification of molecular markers of bipolar cells in the murine retina. J Comp Neurol 507:1795–1810.

Kobayashi M, Takezawa S, Hara K, Yu RT, Umesono Y, Agata K, Taniwaki M, Yasuda K, Umesono K. 1999. Identification of a photoreceptor cell-specific nuclear receptor. Proc Natl Acad Sci U S A 96:4814–4819.

Kreitzer AC, Regehr WG. 2002. Retrograde signaling by endocannabinoids. Curr Opin Neurobiol 12:324–330.

Lalonde MR, Jollimore CA, Stevens K, Barnes S, Kelly ME. 2006. Cannabinoid receptor-mediated inhibition of calcium signaling in rat retinal ganglion cells. Mol Vis 12: 1160–1166.

Leonelli M, Britto LR, Chaves GP, Torrao AS. 2005. Developmental expression of cannabinoid receptors in the chick retinotectal system. Brain Res Dev Brain Res 156:176–182.

Leu S, Ouyang P. 2006. Spatial and temporal expression profile of pinin during mouse development. Gene Expr Patterns 6:620–631.

Li L, Bender KJ, Drew PJ, Jadhav SP, Sylwestrak E, Feldman DE. 2009. Endocannabinoid signaling is required for development and critical period plasticity of the whisker map in somatosensory cortex. Neuron 64:537–549.

Li S, Mo Z, Yang X, Price SM, Shen MM, Xiang M. 2004. Foxn4 controls the genesis of amacrine and horizontal cells by retinal progenitors. Neuron 43:795–807.

Li Y, Zheng H, Liu PP, Chen YY, She ZJ, Xiao HL, Zhou GM. 2010. The new targets of ouabain in retinal interneurons of Sprague-Dawley rats. Brain Res Bull 81:617–624.

Mailleux P, Parmentier M, Vanderhaeghen JJ. 1992. Distribution of cannabinoid receptor messenger RNA in the human brain: an in situ hybridization histochemistry with oligonucleotides. Neurosci Lett 143:200–204.

Malicki J. 2004. Cell fate decisions and patterning in the vertebrate retina: the importance of timing, asymmetry, polarity and waves. Curr Opin Neurobiol 14:15–21.

Marsicano G, Wotjak CT, Azad SC, Bisogno T, Rammes G, Cascio MG, Hermann H, Tang J, Hofmann C, Zieglgansberger W, Di Marzo V, Lutz B. 2002. The endogenous cannabinoid system controls extinction of aversive memories. Nature 418:530–534.

Masland RH, Mills JW, Hayden SA. 1984. Acetylcholine-synthesizing amacrine cells: identification and selective staining by using radioautography and fluorescent markers. Proc R Soc Lond B 223:79–100.

Mayor S, Maxfield FR. 1995. Insolubility and redistribution of GPI-anchored proteins at the cell surface after detergent treatment. Mol Biol Cell 6:929–944.

McGinnis JF, Stepanik PL, Baehr W, Subbaraya I, Lerious V. 1992a. Cloning and sequencing of the 23 kDa mouse photoreceptor cell-specific protein. FEBS Lett 302:172–176.

McGinnis JF, Whelan JP, Donoso LA. 1992b. Transient, cyclic changes in mouse visual cell gene products during the light-dark cycle. J Neurosci Res 31:584–590.

McGinnis JF, Stepanik PL, Jariangprasert S, Lerious V. 1997. Functional significance of recoverin localization in multiple retina cell types. J Neurosci Res 50:487–495.

McKinney MK, Cravatt BF. 2005. Structure and function of fatty acid amide hydrolase. Annu Rev Biochem 74: 411–432.

McLaughlin CR, Abood ME. 1993. Developmental expression of cannabinoid receptor mRNA. Brain Res Dev Brain Res 76:75–78.

McLaughlin T, Torborg CL, Feller MB, O'Leary DD. 2003. Retinotopic map refinement requires spontaneous retinal waves during a brief critical period of development. Neuron 40:1147–1160.

Melan MA, Sluder G. 1992. Redistribution and differential extraction of soluble proteins in permeabilized cultured cells. Implications for immunofluorescence microscopy. J Cell Sci 101:731–743.

Micheva KD, Vallee A, Beaulieu C, Herman IM, Leclerc N. 1998. beta-Actin is confined to structures having high capacity of remodelling in developing and adult rat cerebellum. Eur J Neurosci 10:3785–3798.

Milam AH, Dacey DM, Dizhoor AM. 1993. Recoverin immunoreactivity in mammalian cone bipolar cells. Vis Neurosci 10:1–12.

Mitchell CK, Huang B, Redburn-Johnson DA. 1999. GABA(A) receptor immunoreactivity is transiently expressed in the developing outer retina. Vis Neurosci 16:1083–1088.

Morest DK. 1970. The pattern of neurogenesis in the retina of the rat. Z Anat Entwicklungsgesch 131:45–67.

Morgan JL, Dhingra A, Vardi N, Wong RO. 2006. Axons and dendrites originate from neuroepithelial-like processes of retinal bipolar cells. Nat Neurosci 9:85–92.

Morishita J, Okamoto Y, Tsuboi K, Ueno M, Sakamoto H, Maekawa N, Ueda N. 2005. Regional distribution and age-dependent expression of N-acylphosphatidylethanolamine-hydrolyzing phospholipase D in rat brain. J Neurochem 94: 753–762.

Morrow EM, Chen CM, Cepko CL. 2008. Temporal order of bipolar cell genesis in the neural retina. Neural Dev 3:2.

Mulder J, Aguado T, Keimpema E, Barabas K, Ballester Rosado CJ, Nguyen L, Monory K, Marsicano G, Di Marzo V, Hurd YL, Guillemot F, Mackie K, Lutz B, Guzman M, Lu HC, Galve-Roperh I, Harkany T. 2008. Endocannabinoid signaling controls pyramidal cell specification and long-range axon patterning. Proc Natl Acad Sci U S A 105:8760–8765.

Nag TC, Wadhwa S. 2001. Differential expression of syntaxin-1 and synaptophysin in the developing and adult human retina. J Biosci 26:179–191.

Nagar S, Krishnamoorthy V, Cherukuri P, Jain V, Dhingra NK. 2009. Early remodeling in an inducible animal model of retinal degeneration. Neuroscience 160:517–529.

Negishi K, Kato S, Teranishi T. 1988. Dopamine cells and rod bipolar cells contain protein kinase C-like immunoreactivity in some vertebrate retinas. Neurosci Lett 94: 247–252.

Nicholson DA, Geinisman Y. 2009. Axospinous synaptic subtype-specific differences in structure, size, ionotropic receptor expression, and connectivity in apical dendritic regions of rat hippocampal CA1 pyramidal neurons. J Comp Neurol 512:399–418.

Nucci C, Gasperi V, Tartaglione R, Cerulli A, Terrinoni A, Bari M, De Simone C, Agro AF, Morrone LA, Corasaniti MT, Bagetta G, Maccarrone M. 2007. Involvement of the endocannabinoid system in retinal damage after high intraocular pressure-induced ischemia in rats. Invest Ophthalmol Vis Sci 48:2997–3004.

Okamoto Y, Morishita J, Tsuboi K, Tonai T, Ueda N. 2004. Molecular characterization of a phospholipase D generating

anandamide and its congeners. J Biol Chem 279: 5298–5305.
Ono M, Murakami T, Kudo A, Isshiki M, Sawada H, Segawa A. 2001. Quantitative comparison of anti-fading mounting media for confocal laser scanning microscopy. J Histochem Cytochem 49:305–312.
Pan L, Yang Z, Feng L, Gan L. 2005. Functional equivalence of Brn3 POU-domain transcription factors in mouse retinal neurogenesis. Development 132:703–712.
Perry VH, Henderson Z, Linden R. 1983. Postnatal changes in retinal ganglion cell and optic axon populations in the pigmented rat. J Comp Neurol 219:356–368.
Poche RA, Furuta Y, Chaboissier MC, Schedl A, Behringer RR. 2008. Sox9 is expressed in mouse multipotent retinal progenitor cells and functions in Muller glial cell development. J Comp Neurol 510:237–250.
Porcella A, Maxia C, Gessa GL, Pani L. 2000. The human eye expresses high levels of CB1 cannabinoid receptor mRNA and protein. Eur J Neurosci 12:1123–1127.
Quina LA, Pak W, Lanier J, Banwait P, Gratwick K, Liu Y, Velasquez T, O'Leary DD, Goulding M, Turner EE. 2005. Brn3a-expressing retinal ganglion cells project specifically to thalamocortical and collicular visual pathways. J Neurosci 25:11595–11604.
Rapaport DH, Wong LL, Wood ED, Yasumura D, LaVail MM. 2004. Timing and topography of cell genesis in the rat retina. J Comp Neurol 474:304–324.
Raven MA, Orton NC, Nassar H, Williams GA, Stell WK, Jacobs GH, Bech-Hansen NT, Reese BE. 2008. Early afferent signaling in the outer plexiform layer regulates development of horizontal cell morphology. J Comp Neurol 506:745–758.
Rich KA, Zhan Y, Blanks JC. 1997. Migration and synaptogenesis of cone photoreceptors in the developing mouse retina. J Comp Neurol 388:47–63.
Riepe RE, Norenburg MD. 1977. Muller cell localisation of glutamine synthetase in rat retina. Nature 268:654–655.
Riepe RE, Norenberg MD. 1978. Glutamine synthetase in the developing rat retina: an immunohistochemical study. Exp Eye Res 27:435–444.
Rimmerman N, Hughes HV, Bradshaw HB, Pazos MX, Mackie K, Prieto AL, Walker JM. 2008. Compartmentalization of endocannabinoids into lipid rafts in a dorsal root ganglion cell line. Br J Pharmacol 153:380–389.
Rodriguez de Fonseca F, Ramos JA, Bonnin A, Fernandez-Ruiz JJ. 1993. Presence of cannabinoid binding sites in the brain from early postnatal ages. Neuroreport 4:135–138.
Schnitzer J, Rusoff AC. 1984. Horizontal cells of the mouse retina contain glutamic acid decarboxylase-like immunoreactivity during early developmental stages. J Neurosci 4: 2948–2955.
Schroeter EH, Wong RO, Gregg RG. 2006. In vivo development of retinal ON-bipolar cell axonal terminals visualized in nyx:: MYFP transgenic zebrafish. Vis Neurosci 23:833–843.
Sernagor E, Eglen SJ, O'Donovan MJ. 2000. Differential effects of acetylcholine and glutamate blockade on the spatiotemporal dynamics of retinal waves. J Neurosci 20:RC56.
Sharma RK, O'Leary TE, Fields CM, Johnson DA. 2003. Development of the outer retina in the mouse. Brain Res Dev Brain Res 145:93–105.
Sherry DM, Wang MM, Bates J, Frishman LJ. 2003. Expression of vesicular glutamate transporter 1 in the mouse retina reveals temporal ordering in development of rod vs. cone and ON vs. OFF circuits. J Comp Neurol 465:480–498.
Song ZH, Zhong M. 2000. CB1 cannabinoid receptor-mediated cell migration. J Pharmacol Exp Ther 294:204–209.
Stacy RC, Demas J, Burgess RW, Sanes JR, Wong RO. 2005. Disruption and recovery of patterned retinal activity in the absence of acetylcholine. J Neurosci 25:9347–9357.
Straiker A, Sullivan JM. 2003. Cannabinoid receptor activation differentially modulates ion channels in photoreceptors of the tiger salamander. J Neurophysiol 89:2647–2654.
Straiker A, Stella N, Piomelli D, Mackie K, Karten HJ, Maguire G. 1999. Cannabinoid CB1 receptors and ligands in vertebrate retina: localization and function of an endogenous signaling system. Proc Natl Acad Sci U S A 96:14565–14570.
Struik ML, Yazulla S, Kamermans M. 2006. Cannabinoid agonist WIN 55212-2 speeds up the cone response to light offset in goldfish retina. Vis Neurosci 23:285–293.
Suarez J, Bermudez-Silva FJ, Mackie K, Ledent C, Zimmer A, Cravatt BF, de Fonseca FR. 2008. Immunohistochemical description of the endogenous cannabinoid system in the rat cerebellum and functionally related nuclei. J Comp Neurol 509:400–421.
Suarez J, Romero-Zerbo SY, Rivera P, Bermudez-Silva FJ, Perez J, De Fonseca FR, Fernandez-Llebrez P. 2010. Endocannabinoid system in the adult rat circumventricular areas: an immunohistochemical study. J Comp Neurol 518: 3065–3085.
Syed MM, Lee S, Zheng J, Zhou ZJ. 2004. Stage-dependent dynamics and modulation of spontaneous waves in the developing rabbit retina. J Physiol 560:533–549.
Tauchi M, Masland RH. 1984. The shape and arrangement of the cholinergic neurons in the rabbit retina. Proc R Soc Lond B 223:101–119.
Thomas EA, Cravatt BF, Danielson PE, Gilula NB, Sutcliffe JG. 1997. Fatty acid amide hydrolase, the degradative enzyme for anandamide and oleamide, has selective distribution in neurons within the rat central nervous system. J Neurosci Res 50:1047–1052.
Torborg CL, Feller MB. 2005. Spontaneous patterned retinal activity and the refinement of retinal projections. Prog Neurobiol 76:213–235.
Turu G, Hunyady L. Signal transduction of the CB1 cannabinoid receptor. J Mol Endocrinol 44:75–85.
Voinescu PE, Kay JN, Sanes JR. 2009. Birthdays of retinal amacrine cell subtypes are systematically related to their molecular identity and soma position. J Comp Neurol 517: 737–750.
Wang H, Xie H, Sun X, Kingsley PJ, Marnett LJ, Cravatt BF, Dey SK. 2007. Differential regulation of endocannabinoid synthesis and degradation in the uterus during embryo implantation. Prostaglandins Other Lipid Mediat 83:62–74.
Warrier A, Wilson M. 2007. Endocannabinoid signaling regulates spontaneous transmitter release from embryonic retinal amacrine cells. Vis Neurosci 24:25–35.
Waseem NH, Lane DP. 1990. Monoclonal antibody analysis of the proliferating cell nuclear antigen (PCNA). Structural conservation and the detection of a nucleolar form. J Cell Sci 96:121–129.
Weinberger R, Schevzov G, Jeffrey P, Gordon K, Hill M, Gunning P. 1996. The molecular composition of neuronal microfilaments is spatially and temporally regulated. J Neurosci 16:238–252.
Westlake TM, Howlett AC, Bonner TI, Matsuda LA, Herkenham M. 1994. Cannabinoid receptor binding and messenger RNA expression in human brain: an in vitro receptor autoradiography and in situ hybridization histochemistry study of normal aged and Alzheimer's brains. Neuroscience 63: 637–652.
Williams EJ, Walsh FS, Doherty P. 2003. The FGF receptor uses the endocannabinoid signaling system to couple to an axonal growth response. J Cell Biol 160:481–486.
Wong WT, Myhr KL, Miller ED, Wong RO. 2000. Developmental changes in the neurotransmitter regulation of correlated spontaneous retinal activity. J Neurosci 20:351–360.

Xue J, Li G, Laabich A, Cooper NG. 2001. Visual-mediated regulation of retinal CaMKII and its GluR1 substrate is age-dependent. Brain Res Mol Brain Res 93:95–104.

Yan XX, Wiechmann AF. 1997. Early expression of recoverin in a unique population of neurons in the human retina. Anat Embryol (Berl) 195:51–63.

Yazulla S. 2008. Endocannabinoids in the retina: from marijuana to neuroprotection. Prog Retin Eye Res 27:501–526.

Yazulla S, Studholme KM, McIntosh HH, Deutsch DG. 1999. Immunocytochemical localization of cannabinoid CB1 receptor and fatty acid amide hydrolase in rat retina. J Comp Neurol. 1999;12:80–90.

Yazulla S, Studholme KM, McIntosh HH, Fan SF. 2000. Cannabinoid receptors on goldfish retinal bipolar cells: electron-microscope immunocytochemistry and whole-cell recordings. Vis Neurosci 17:391–401.

Zabouri N, Bouchard J-F, Casanova C. 2007. Expression of the endocannabinoid receptor CB1 and the FAAH enzyme during retinal development in the rat. Program No. 461.23/F39 Neuroscience (2007) Abstracts. San Diego, CA: Society for Neuroscience.

Zabouri N, Bouchard J-F, Casanova C. Expression of the NAPE-PLD, CB1 receptors, and FAAH during retinal development. Program No. 723.15/C19. Neuroscience (2008) Abstracts. Washington, DC: Society for Neuroscience.

Zheng J, Lee S, Zhou ZJ. 2006. A transient network of intrinsically bursting starburst cells underlies the generation of retinal waves. Nat Neurosci 9:363–371.

Zhou ZJ. 1998. Direct participation of starburst amacrine cells in spontaneous rhythmic activities in the developing mammalian retina. J Neurosci 18:4155–4165.

Zhou ZJ, Zhao D. 2000. Coordinated transitions in neurotransmitter systems for the initiation and propagation of spontaneous retinal waves. J Neurosci 20:6570–6577.